NAVAL POSTGRADUATE SCHOOL

MONTEREY, CALIFORNIA

THESIS

LASER VELOCIMETRIC FLOW MAPPING AND CHARACTERIZATION OF OIL MIST NOZZLES USED FOR BLADE EXCITATION IN HIGH CYCLE FATIGUE TESTING

by

Christopher M. Vonderheide

September 2005

Thesis Advisor: Raymond Shreeve
Second Reader: Garth Hobson

THIS PAGE INTENTIONALLY LEFT BLANK

REPORT DOCUMENTATION PAGE			*Form Approved OMB No. 0704-0188*

1. AGENCY USE ONLY ***(Leave blank)***	**2. REPORT DATE** September 05	**3. REPORT TYPE AND DATES COVERED** Master's Thesis

4. TITLE AND SUBTITLE: Laser Velocimetric Flow Mapping and Characterization of Oil Mist Nozzles Used for Blade Excitation in High Cycle Fatigue Testing	**5. FUNDING NUMBERS**
6. AUTHOR(S) Christopher M. Vonderheide	
7. PERFORMING ORGANIZATION NAME(S) AND ADDRESS(ES) Naval Postgraduate School Monterey, CA 93943-5000	**8. PERFORMING ORGANIZATION REPORT NUMBER**
9. SPONSORING /MONITORING AGENCY NAME(S) AND ADDRESS(ES) N/A	**10. SPONSORING/MONITORING AGENCY REPORT NUMBER**

11. SUPPLEMENTARY NOTES The views expressed in this thesis are those of the author and do not reflect the official policy or position of the Department of Defense or the U.S. Government.

12a. DISTRIBUTION / AVAILABILITY STATEMENT Approved for public release; distribution unlimited.	**12b. DISTRIBUTION CODE**

13. ABSTRACT (maximum 200 words)

The flow patterns of two oil mist nozzles used in rotor blade excitation experiments were flow mapped using a traversing Laser Doppler Velocimeter (LDV) system to determine the velocity and the overall characteristics were recorded photographically. The nozzles were operated in a vacuum test chamber and measurements were obtained at three different spray pressures, at three different axial distances from the nozzle exit. For a 4 gallon per hour (gph) "mini-mist" nozzle, a 'referenced velocity' was defined which was found to be constant within a hollow cone, and the cone geometry and oil flow rate changed linearly with the oil supply pressure. A 6 gph "standard" nozzle gave a solid cone, but only gave a pattern free of liquid streaks at low pressures. Oil temperature affected this behavior. The analytic quantification of the spray pattern can be used to design specific blade excitation experiments in high cycle fatigue (HCF) vacuum spin tests.

14. SUBJECT TERMS: Oil jet excitation, Mist nozzle, Laser Doppler velocimetry, Rotor spin pit, High cycle fatigue, Blade excitation.	**15. NUMBER OF PAGES** 79
	16. PRICE CODE

17. SECURITY CLASSIFICATION OF REPORT	**18. SECURITY CLASSIFICATION OF THIS PAGE**	**19. SECURITY CLASSIFICATION OF ABSTRACT**	**20. LIMITATION OF ABSTRACT**
Unclassified	Unclassified	Unclassified	UL

NSN 7540-01-280-5500 Standard Form 298 (Rev. 2-89)
Prescribed by ANSI Std. 239-18

THIS PAGE INTENTIONALLY LEFT BLANK

LASER VELOCIMETRIC FLOW MAPPING AND CHARACTERIZATION OF OIL MIST NOZZLES USED FOR BLADE EXCITATION IN HIGH CYCLE FATIGUE TESTING

Christopher M. Vonderheide
Ensign, United States Navy Reserve
B.S., United States Naval Academy 2004

Submitted in partial fulfillment of the
requirements for the degree of

MASTER OF SCIENCE IN MECHANICAL ENGINEERING

from the

NAVAL POSTGRADUATE SCHOOL
September 2005

Author: Christopher M. Vonderheide

Approved by: Dr. Raymond Shreeve
Thesis Advisor

Dr. Garth Hobson
Second Reader/Co-Advisor

Dr. Anthony Healey
Chairman, Department of Mechanical and Astronautical Engineering

THIS PAGE INTENTIONALLY LEFT BLANK

ABSTRACT

The flow patterns of two oil mist nozzles used in rotor blade excitation experiments were flow mapped using a traversing Laser Doppler Velocimeter (LDV) system to determine the velocity and the overall characteristics were recorded photographically. The nozzles were operated in a vacuum test chamber and measurements were obtained at three different spray pressures, at three different axial distances from the nozzle exit. For a 4 gallon per hour (gph) "mini-mist" nozzle, a 'referenced velocity' was defined which was found to be constant within a hollow cone, and the cone geometry and oil flow rate changed linearly with the oil supply pressure. A 6 gph "standard" nozzle gave a solid cone, but only gave a pattern free of liquid streaks at low pressures. Oil temperature affected this behavior. The analytic quantification of the spray pattern can be used to design specific blade excitation experiments in high cycle fatigue (HCF) vacuum spin tests.

THIS PAGE INTENTIONALLY LEFT BLANK

TABLE OF CONTENTS

THIS PAGE INTENTIONALLY LEFT BLANK

LIST OF FIGURES

THIS PAGE INTENTIONALLY LEFT BLANK

LIST OF TABLES

THIS PAGE INTENTIONALLY LEFT BLANK

ACKNOWLEDGMENTS

I would like to thank Dr Raymond Shreeve for his guidance and patience. I am thankful for the opportunity to have worked with him. His encouragement was essential to getting me through those times when I was less than confident.

I would like to thank Dr Garth Hobson for showing me how to use the Laser Doppler Velocimeter, and helping me work through the little problems I encountered with it along the way. Without the use of the LDV, my studies would not have been possible.

I would like to thank Rick Still and John Gibson because without them my experiments could not have been done. They modified the test apparatus numerous times and showed me how to use it after each. They made me feel welcome at the laboratory and made time spent there a little less like work.

Finally, I'd like to thank my fiancée Heidi Zomermaand for her support. She always lent a sympathetic ear and provided kind words when I needed them most. She kept me on track with her questions and was always gracious enough to let me know when I needed to work a little harder.

THIS PAGE INTENTIONALLY LEFT BLANK

I. INTRODUCTION

In recent years, due to a heightened awareness of 'durability' in developing advanced military aircraft engines, oil jet excitation (OJE) has been used successfully to excite rotor blade resonance in vacuum spin tests (References 1, 2). Such tests are conducted to evaluate proposed damping techniques, to validate new blading designs and to investigate high cycle fatigue (HCF) tolerance to blade damage. The OJE technique has emerged as the only technique which can, in principle, be used continuously to produce excitation forces large enough at resonance to prove HCF endurance to 10^7 cycles. Alternate excitation methods degrade the vacuum (air jet excitation), result in excessive heating (eddy-current excitation) or do not produce adequate excitation amplitudes (piezo-electric excitation).

Early experience with OJE showed that discrete oil jets gave large excitation magnitudes but that the 'erosion threshold' would be passed before a 10^7 cycle test would be completed (Reference 1). In comparison, commercial oil-mist nozzles, similarly arranged, gave lower excitation amplitudes. Consequently, studies were initiated to both extend the erosion threshold by using discrete jets having much smaller diameters, and improve the excitation amplitudes obtained using mist nozzles by improving positioning and controlling the oil penetration into the rotor's path. The development of practical discrete jet nozzles having much smaller diameters was reported by Moreno (Reference 3). When it was found in spin pit testing that oil-mist nozzles could indeed produce sufficiently high amplitudes for endurance testing (Reference 2), attention was re-directed at being able to design oil-mist injection systems optimally, to excite any given mode of vibration in any new rotor test.

Therefore, the goal of the present study was to characterize and quantify the spray patterns of commercial oil spray nozzles currently used in vacuum spin tests. Two specific nozzles were selected. First, a four gallon per hour "mini-mist" Hago nozzle typical of those used in the Rotor Spin Research Facility at the Naval Postgraduate School (NPS), and second a six gallon per hour "standard" Hago nozzle typical of those used in the Rotor Spin Facility at the Naval Air Warfare Center's Propulsion and Power

Center at Patuxent River, Maryland. The NPS program is an integral part of the U.S. Navy's program directed from Patuxent River.

II. BACKGROUND

A. ROTOR SPIN RESEARCH FACILITY

The Rotor Spin Research Facility was established at the Turbopropulsion Laboratory at NPS to support the HCF testing program at the Naval Air Systems Command's facility at Patuxent River in Maryland. Figure 1 shows the spin pit in Building 215 at TPL. It shows the apparatus in a partially disassembled state, with the test rotor lifted out of the pit itself. Figure 2 is a cross sectional view of the spin pit showing its material construction.

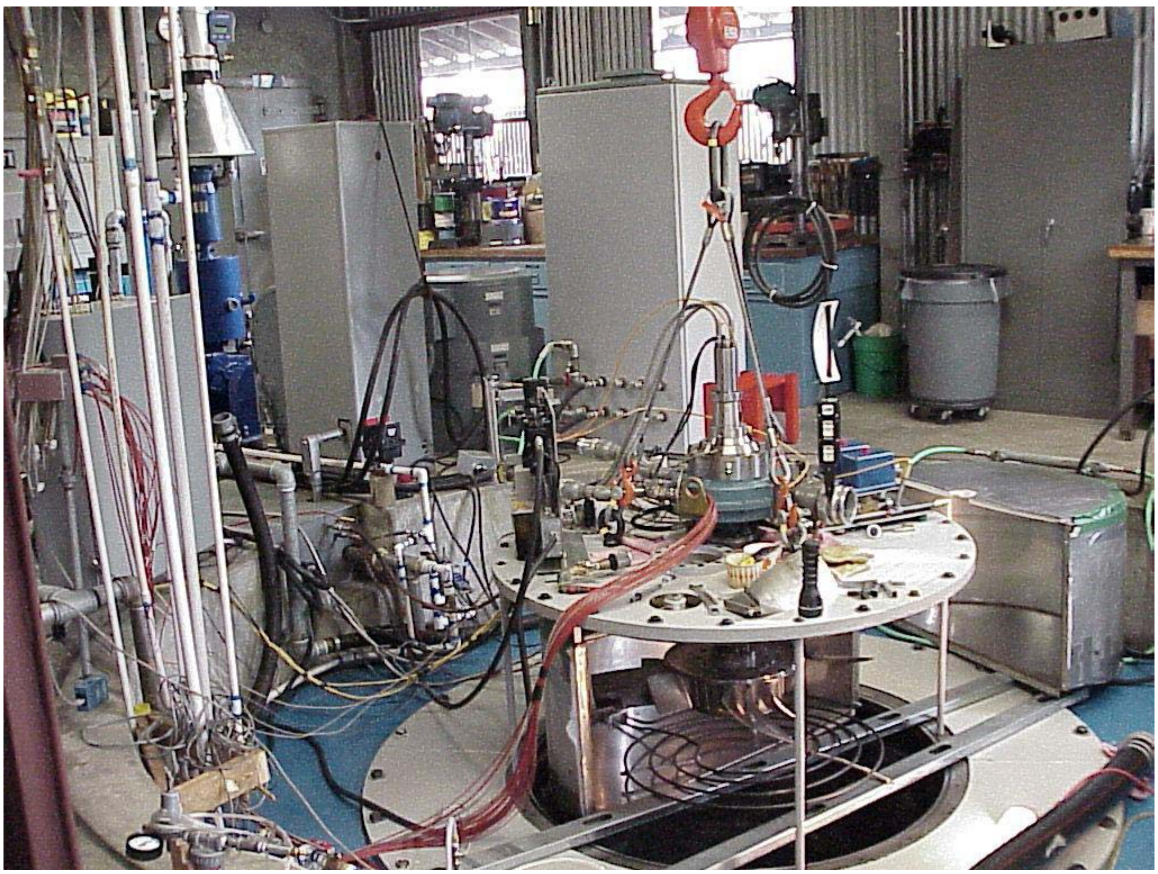

Figure 1. Spin pit at Naval Postgraduate School Turbopropulsion Laboratory.

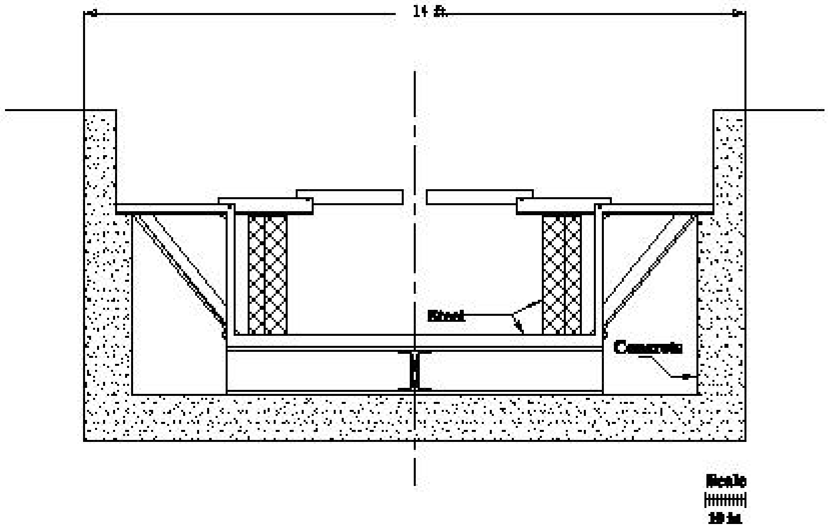

Figure 2. TPL spin pit cross section.

The test rotor hangs in the pit and is driven by an air turbine. During experiments the pit is maintained at a near vacuum. This allows the air turbine to drive the blade at very high speeds using a small amount of energy. With no air to interact with the test rotor, a method of exciting the blade is required. This has been done successfully using oil injection methods, particularly the oil-mist nozzles described later.

The oil system diagram for the TPL spin pit facility is shown in Figure 3. The position of pumps, valves, and the layout of the injection recovery system is visible. Figure 4 shows a typical arrangement of mist nozzles in the spin pit, with the nozzles spaced radially around the pit and under the rotor so that their spray will impact the undersurface of the blade tips. A series of strain gauges measures the blade's response to the oil impact.

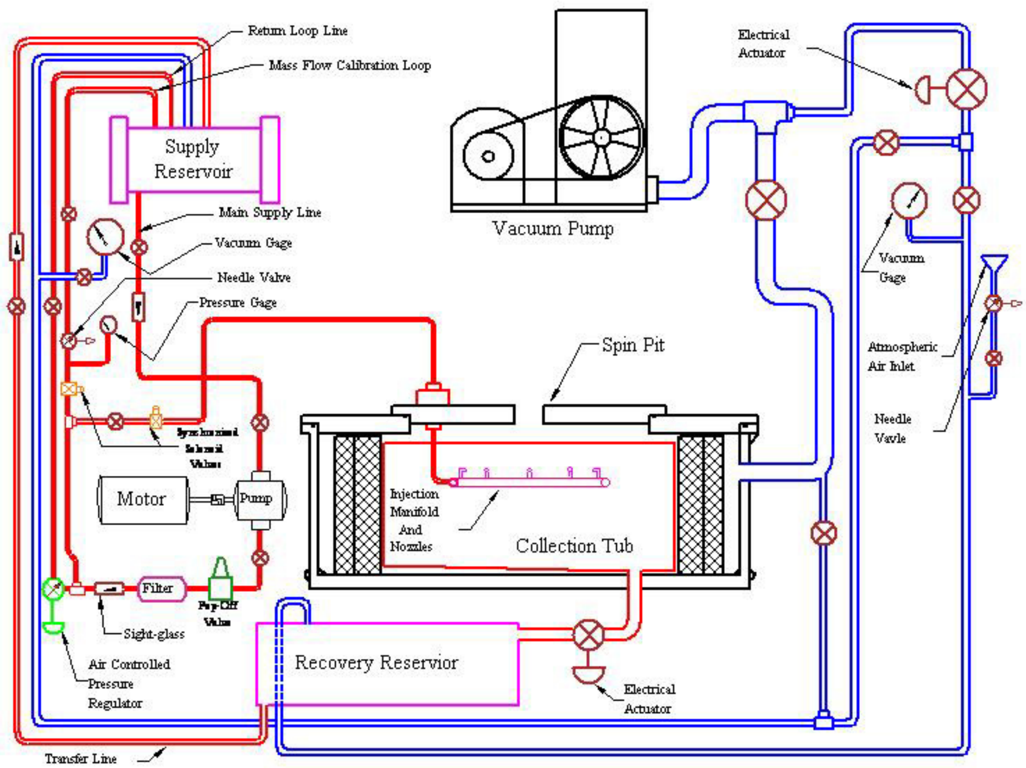

Figure 3. Spin pit oil injection and recovery system diagram.

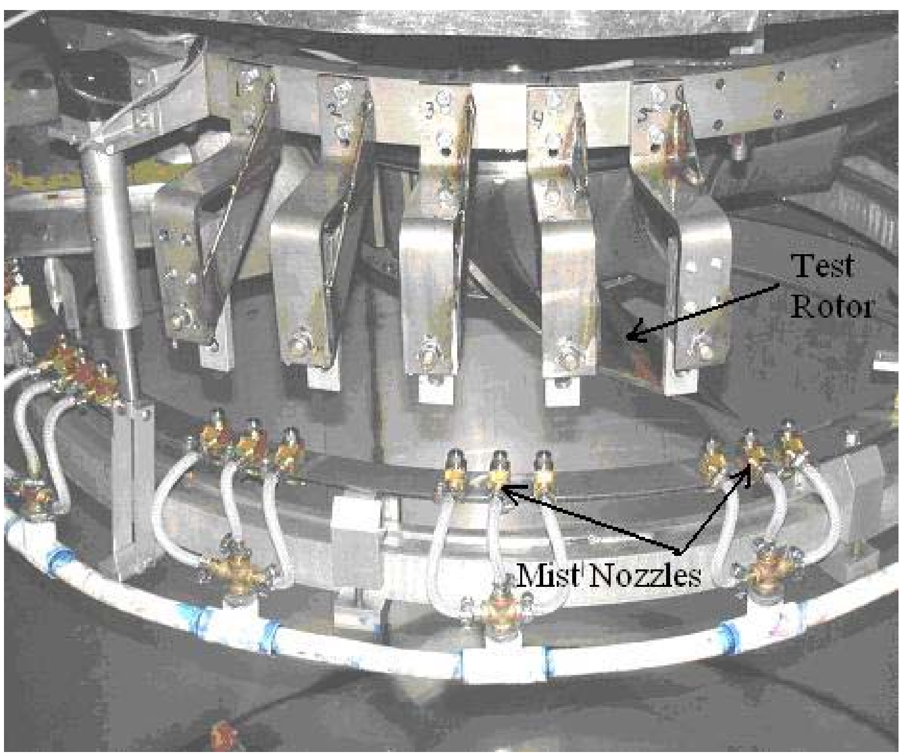

Figure 4. Test rotor and typical arrangement of oil-mist nozzles.

B. APPROACH

In early tests, the focus was on discrete oil jets as mist nozzles did not provide the vibration amplitudes required (Reference 1). It was discovered subsequently that while the discrete jets provided ample vibration, they also caused erosion of the metal blade surface after a period of time. A full description of the erosion phenomenon can be found in Moreno (Reference 3). In order to eliminate the metal erosion a series of very small discrete jets was manufactured and tested in a vacuum chamber. To date the erosion characteristics of the small discrete jets have not been evaluated by testing in the spin pit.

Mist nozzles were expected not to erode the blade surface and so tests were re-designed to increase the vibration amplitude achieved with them. When these were successful (Reference 3), it became important to be able to quantify the spray patterns precisely in order to facilitate the design of any new excitation requirement. Illustrations of the excitation problem are shown in Figures 5 and 6. Figure 5 shows the radial view of the rotor blade from Figure 4 and penetration of the oil spray following one, six, or eleven empty blade spaces in a partially bladed rotor. Figure 6 shows the spread of the oil across the blade surface, on which is also shown the modal lines of the targeted oscillation. (The discrete jet pattern shown was form oil jets discharging radially inwards, which is not shown in Figure 4.)

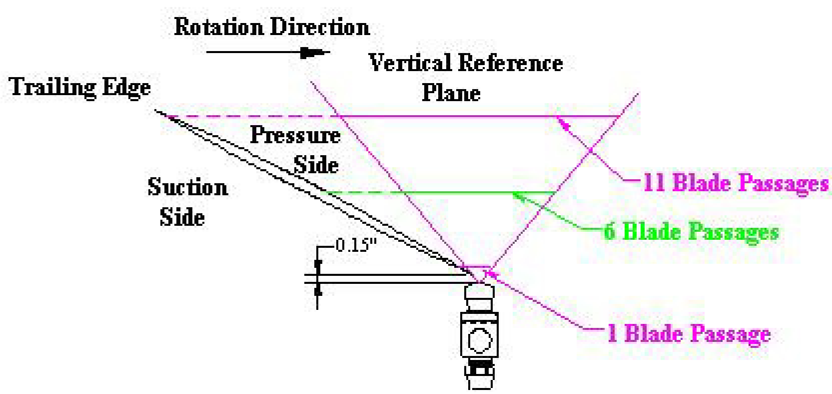

Figure 5. Radial view of rotor blade showing oil penetration distance.

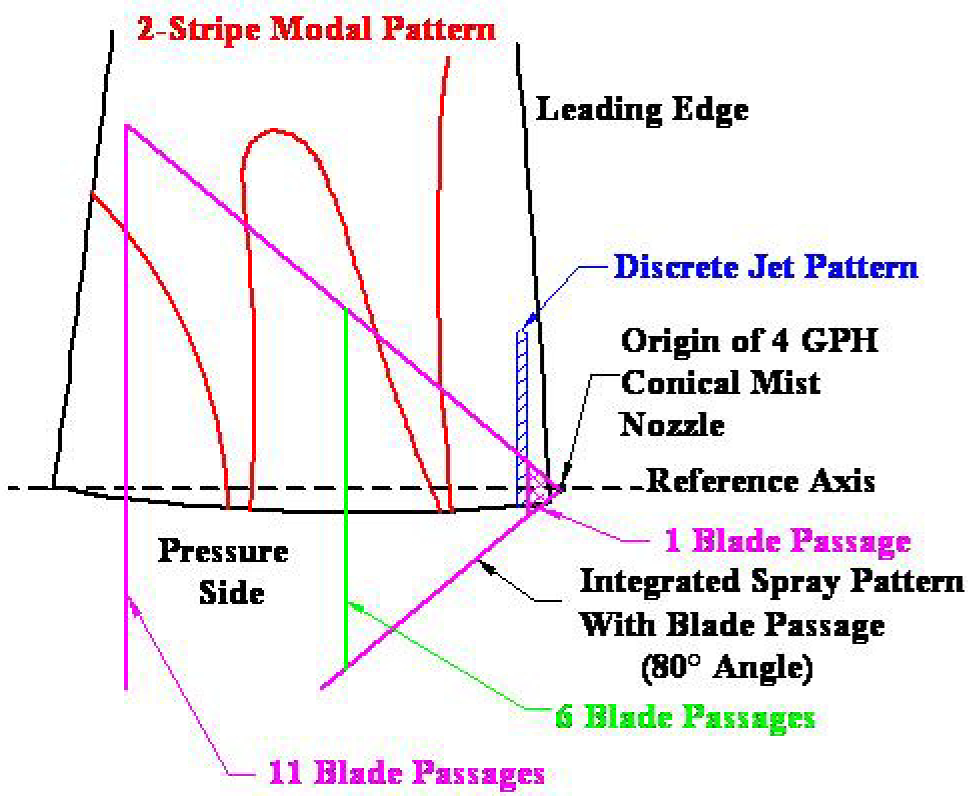

Figure 6. Blade surface showing oil spread and example modal lines.

In order to construct these oil mist patterns, both the velocity of the oil droplets and the area of spread are required. Such information was not provided by the nozzle manufacturers, and will likely depend on the properties of the particular oil being used. Even if the spray was modeled as a straight hollow cone, the velocity could not be derived from the mass flow rate unless the particle concentration and size were both known.

Therefore, a direct mapping of the velocity was a primary requirement, and early results led to establishing and measuring the parameters shown in Figure 7. The goal was to describe these characteristic parameters in terms of the nozzle flow pressure only. With the oil mass flow rate, these are the parameters that are required to be able to determine the force that will be imparted on the rotating blade by the oil. The rotor velocity and flow rate are required to determine the momentum the oil will have when it hits the blade and the mass of oil that will be present above the nozzle for each blade pass. The critical angles are needed to determine the area over which this force will be distributed, and the oil concentration in that area.

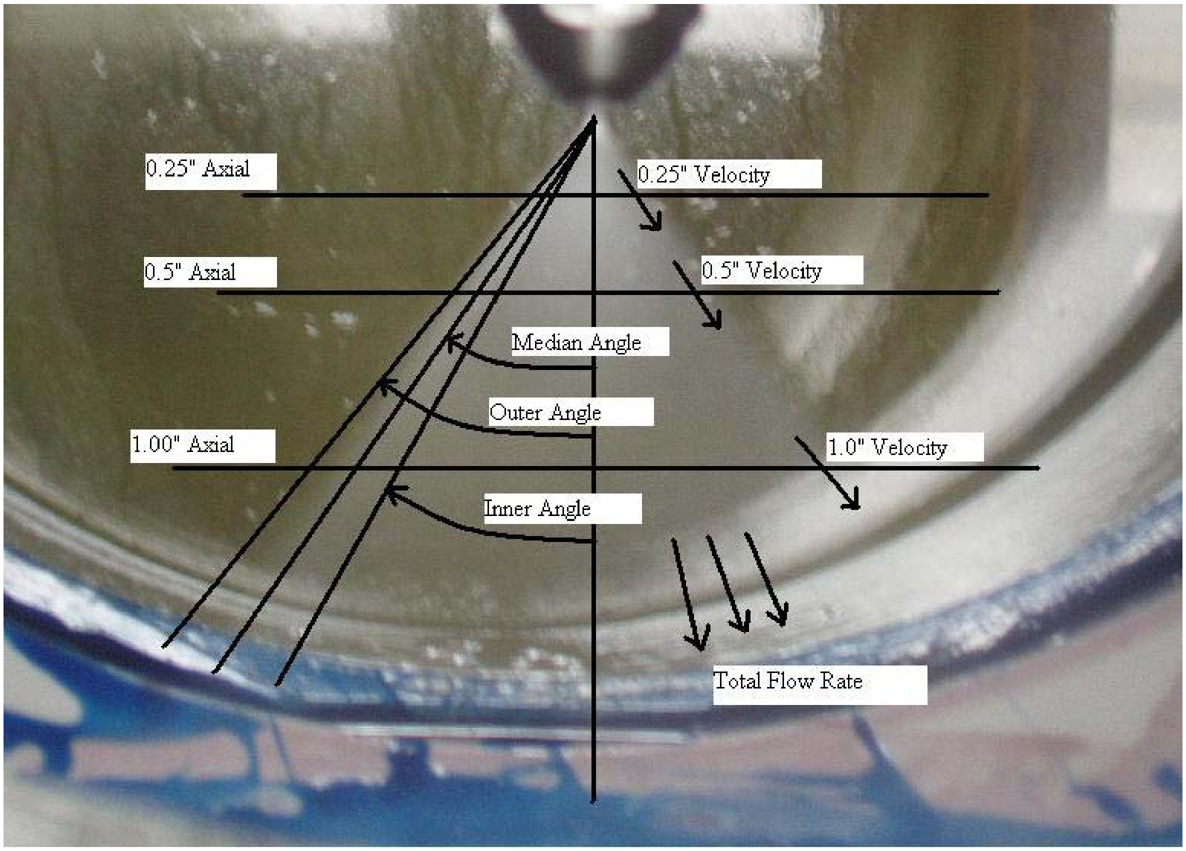

Figure 7. Required parameters for mist nozzle description.

III. APPARATUS AND PROCEDURE

A. APPARATUS DESCRIPTION

1. Vacuum Test Chamber

The vacuum test chamber is shown in Figure 8. This view shows the test chamber, oil reservoir, and piping. The apparatus was built largely from PVC piping by the technicians at TPL. Several modifications were made to the test chamber based on Moreno's recommendations (Reference 3).

Figure 8. Side view of the vacuum chamber setup.

The first was that the chamber was turned so that the wand and nozzle were perpendicular to the floor, shown in Figure 9. This eliminated the need for an angle rotation to velocity measurements that had to be made previously. Other modifications were very minor but included a revised oil recovery system.

Figure 9. End view of the vacuum chamber showing windows and oil reservoir.

The oil used with the mist nozzles remained the MARCOL 5 produced by Exxon Mobil. It was essentially a very light mineral oil. The Material Safety Data Sheets (MSDS) for the oil can be found in Appendix A.

2. LDV System

The droplet velocities for the mist nozzles were measured using a Laser Doppler Velocimeter (LDV) manufactured by TSI incorporated (Reference 4). Figure 10 shows the laser on its traverse mechanism.

The LDV system used included two sets of two laser beams. One set was aligned horizontally and the other vertically. This allowed the measurement of horizontal and vertical velocity components of the fluid particles. The principle behind an LDV is as follows: a set of two parallel laser beams are split from the same source, and are focused by a lens to cross at a distance from the lens. A pattern of interference fringes is produced within the beam crossing due to the angle of the beams. The fringe separation can be determined from the beam crossing angle and wavelength of light in the beams. As a particle passes through the beam crossing it creates a light and dark return seen by the detector. Because the fringe spacing at the crossing is known, the frequency derived from the reflected signal is a measure of the particle's velocity. By using two pairs of two beams, crossing at right angles, two components of velocity can be obtained from the same measurement volume.

Figure 10. LDV system showing laser and traverse mechanism.

The LDV system was used with the vacuum test chamber as shown in Figure 11. Data acquisition was computer controlled; however, traversing of the laser was done manually.

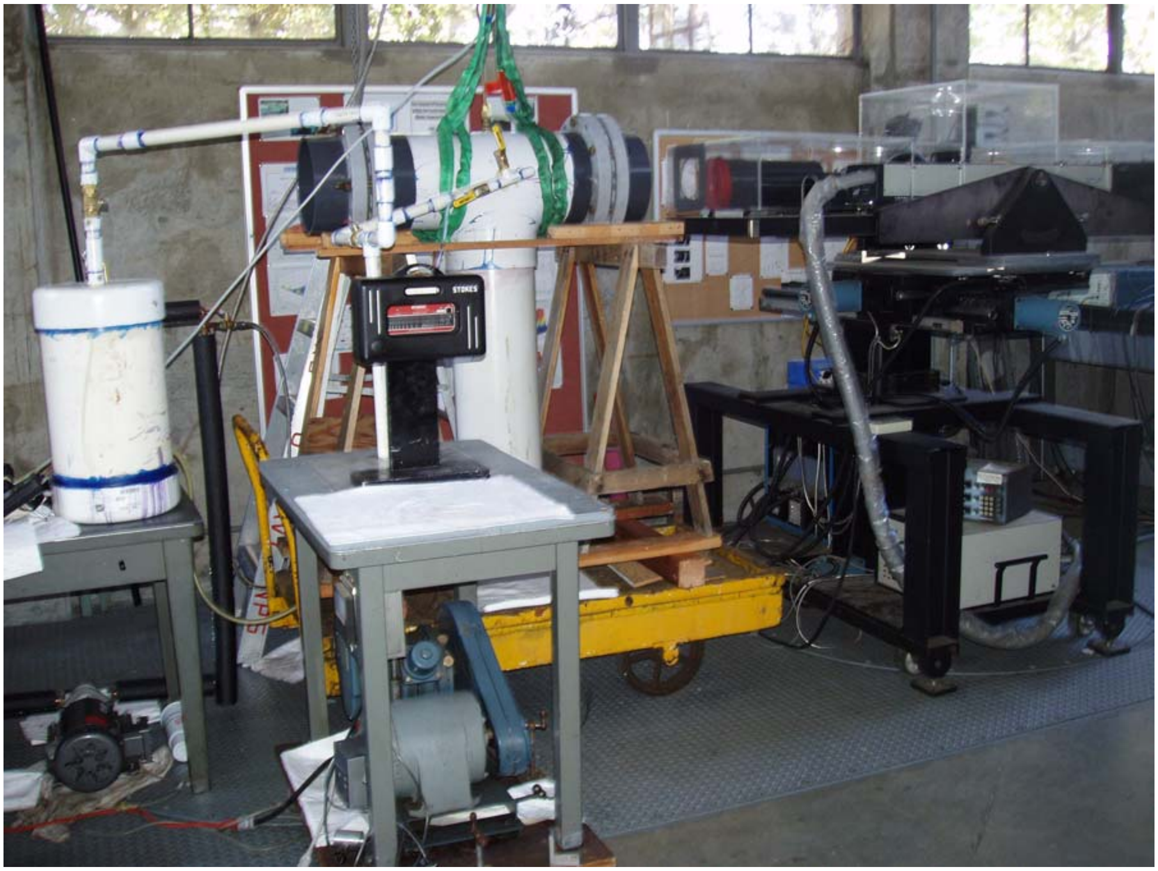

Figure 11. View of LDV system with the vacuum chamber.

B. FLOW MAPPING TECHNIQUE

Before running a survey of an oil-mist nozzle, two important steps were found to be important. First was to let the oil warm up by turning on the pump and allowing friction to bring the oil temperature to a steady value. Without the ability to control the temperature directly, it was necessary to let it stabilize before attempting a survey or viscosity changes could affect the results. The second was to orient the laser. Due to the lack of rigidity in the vacuum chamber's support and the frequency of moving it, the laser had to be repositioned on the nozzle tip. This ensured that the measurement volume would be properly located with respect to the nozzle during the run. The adjustment was made visually using manual control the of laser traverse system, resulting in an estimated uncertainty of 0.05 inches in the recorded position of the data points.

With the system stable, a survey consisted of traversing the laser horizontally through the flow at a constant axial position. A set number of points were taken across the flow with the interval based on the cone width. Data points were described as an "x position," "x velocity," and "z velocity." These three quantities allowed the total velocity of oil droplets, and the flow direction angle from the vertical axis to be calculated. Each nozzle was mapped at three axial (z) positions, as shown in Figure 7, and at three gauge pressures: 60, 80, and 100 psig. The pressures were measured from a gauge located at the base of the 0.5" diameter wand, about 30 inches upstream of the nozzle.

THIS PAGE INTENTIONALLY LEFT BLANK

IV. EXPERIMENTAL RESULTS

A. FOUR GALLON PER HOUR NOZZLE

The Hago 4 gallon per hour (gph) “mini mist” nozzle was tested by LT Moreno and found to possess flow qualities suitable for blade excitation applications. This nozzle was examined first because of its consistent flow behavior. The flow structure was very conical and uniform. The nozzle produced a fine mist over a wide range of pressures. It was also found that temperature fluctuations had a very small impact on its performance. Three surveys were taken with an average oil temperature of about 90 degrees Fahrenheit with a variance of only two to three degrees. Figure 12 shows the total velocity of the 4 gph nozzle at 60 psig. The three axial positions are shown.

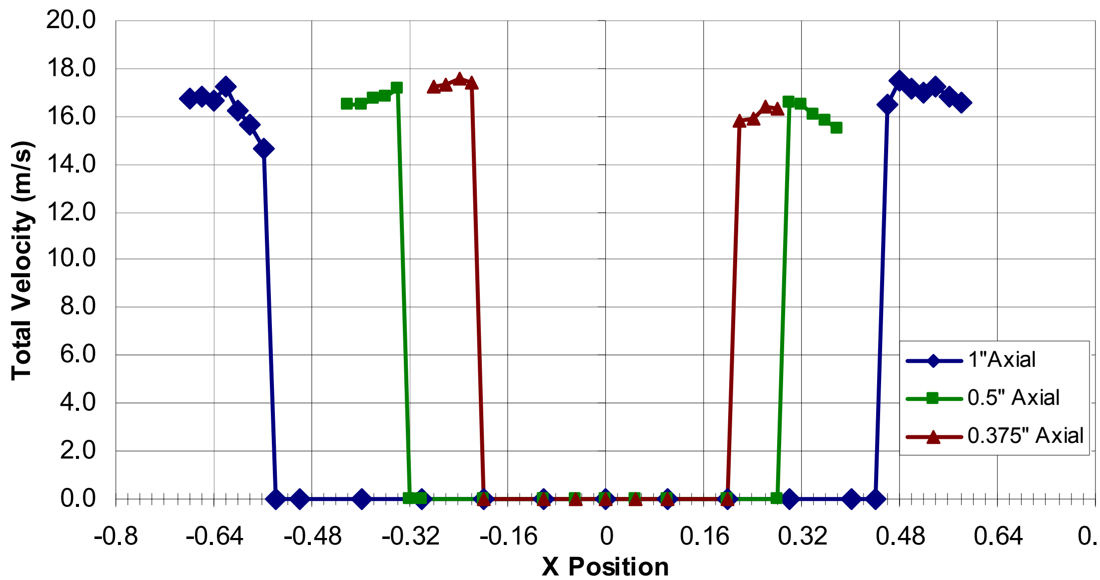

Figure 12. Flow map: 4 gph, 60 psig.

Of note, are the hollow structure of the mist cone and the varying thickness of the cone with axial position. Unfortunately, the very small width of the cone near the nozzle resulted in the saturation of the laser at the 0.25” axial position, with reliable data taken at the 0.375” position instead. The hollow geometry of the mist spray required a new method of survey. Instead of a set number of points, a set interval was chosen. Starting at the edge of the spray measurements were taken at 0.02” horizontal intervals until the data rate dropped off sharply, indicating the hollow interior of the spray.

Figure 13 shows a similar plot at 80 psig. Again, the 0.25” axial position was discarded in favor of reliable results from a 0.375” axial position. Figure 14 is the map of the nozzle at 100 psig.

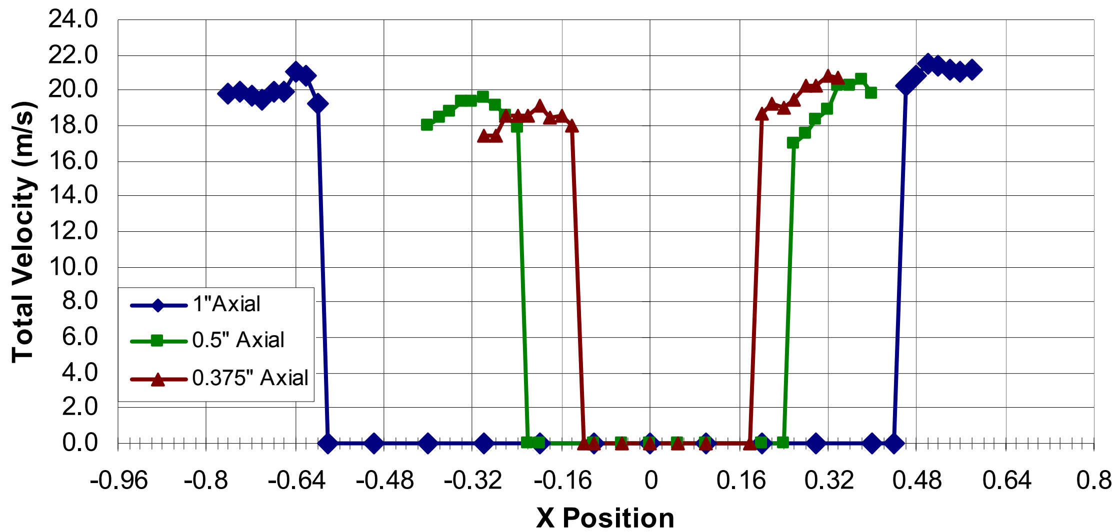

Figure 13. Flow map: 4 gph, 80 psig.

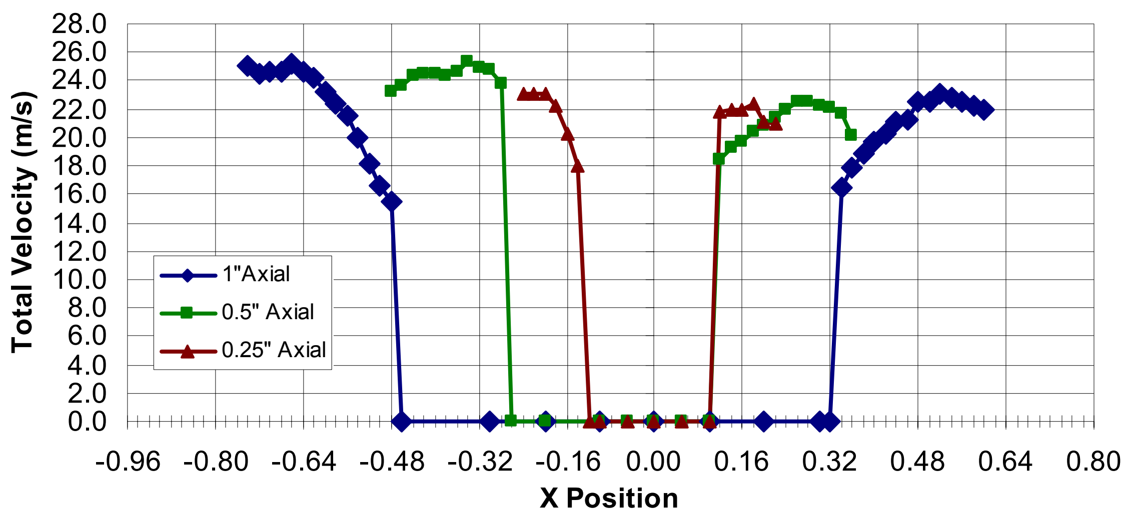

Figure 14. Flow map: 4 gph, 100 psig.

Comparison of the three plots shows that the flow velocities were highest at the outer edge of the cone and decreased towards the inner edge of the flow region. Also, the maximum velocities were fairly constant at the three axial positions for a given pressure.

The three plots also show a continuing increase in the width of the mist cone as the pressure was increased. This is denoted by the increasing number of data points taken at each axial position with increasing pressure. Figure 15 shows a plot of the cone angles derived from the mapped data. The constant average angle of the flow is of importance as is the seemingly linear increase and decrease of the maximum and minimum angles, respectively.

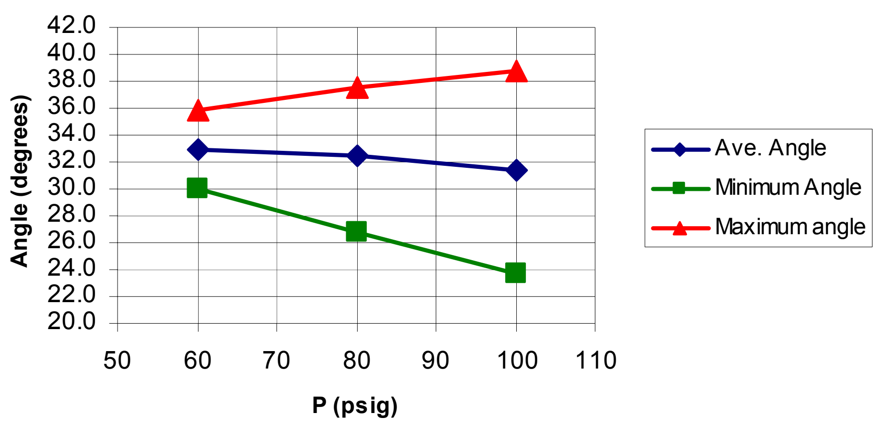

Figure 15. Critical flow angles with varying supply pressure (4 gph).

The flow rate of the 4 gph nozzle was also measured. The Hago mini mist nozzles were characterized by the manufacturer using water. The MARCOL 5 has a different viscosity and thus will flow from the nozzle at a different rate. The flow rate was measured two ways. The first was by weighing the oil that was sprayed over a set time. With the density of the oil known, the flow rate was calculated in gallons per hour. The second was to measure the time taken to spray a set weight of oil. Both methods gave the same results to within the measurement uncertainty. Special attention was paid to the temperature of the oil, ensuring that it was the same as during the LDV surveys to eliminate any effect of density or viscosity change with temperature. Figure 16 shows the flow rates obtained at the three pressures tested. The flow rate measurements were made by spraying into the atmosphere, as opposed to a vacuum, so the data was plotted against total pressure, not gauge pressure. A trend line was added to show the linearity of the data.

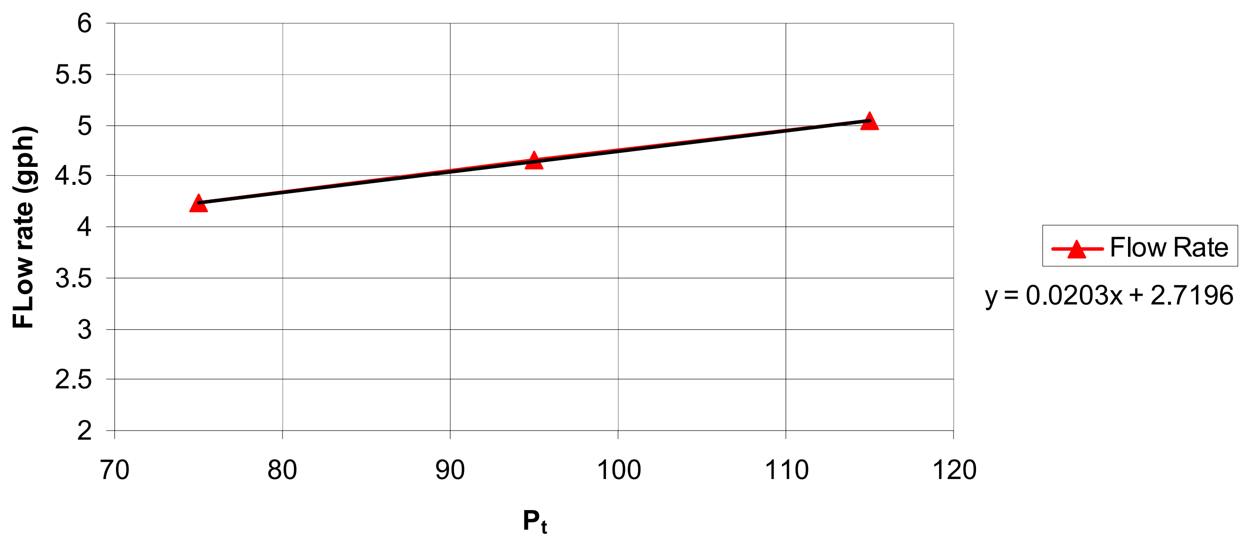

Figure 16. Measured flow rates at various pressures (4 gph nozzle)

B. SIX GALLON PER HOUR NOZZLE

The six gallon per hour nozzle tested was the "standard" Hago nozzle of the type used at the NAWC-AD facility in Patuxent River, Maryland. When previously tested, this nozzle was observed to have a non-uniform flow structure, with streaks of oil present in the mist. The streaks constitute discrete oil jets of inconsistent width and positioning, and this could lead to erosion of the blade surface if used for blade excitation.

The 6 gph nozzle was tested at the same three gauge pressures as the 4 gph nozzle, and due to its higher flow rate the steady temperature of the system was about 80 degrees Fahrenheit, again with a variance of about two to three degrees. Figure 17 shows the total velocity flow map of the 6 gph nozzle at 60 psig at three axial positions. Immediately apparent is that this spray nozzle did not exhibit a hollow cone geometry. In fact, the vertical component of velocity was nearly constant across the entire flow region at a given axial position. At this pressure the flow also seemed to exhibit a fairly symmetric structure.

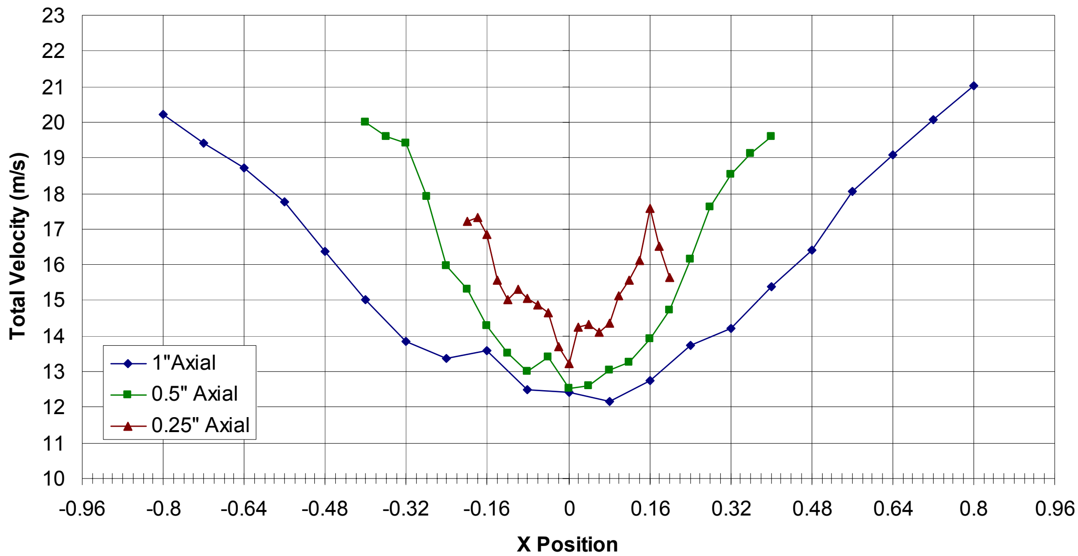

Figure 17. Flow map: 6gph, 60 psig.

This symmetry and apparent steady behavior are not apparent at 80 psig as shown in Figure 18. Instead the velocities were very erratic, with streaks represented by spikes in the velocity curves. Figure 19 shows the flow map for the 6 gph nozzle at 100 psig. Again the non-uniform, irregular structure of the flow is apparent.

Comparison of the three plots shows that there was a larger variance in the velocities at the three axial positions for a given pressure than with the 4 gph nozzle. Also, the non-uniformity of the flow seems to be affected by the flow pressure. The 60 psig flow pattern exhibits a well-behaved, steady structure while the 80 and 100 psig flow patterns do not.

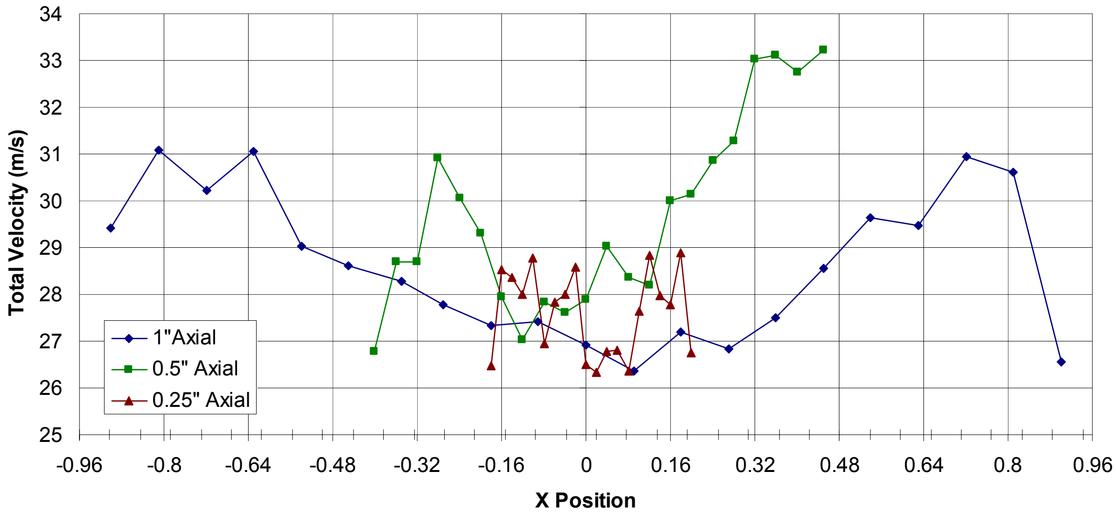

Figure 18. Flow map: 6gph, 80 psig.

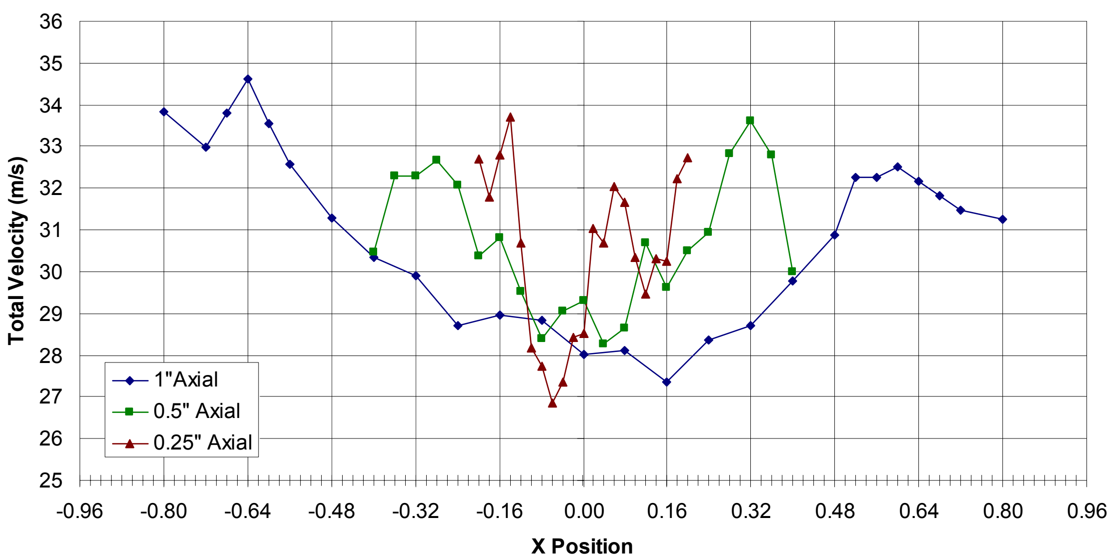

Figure 19. Flow map: 6gph, 100 psig.

V. DATA ANALYSIS

A. FOUR GALLON PER HOUR NOZZLE

1. Velocity Reduction

After mapping the two nozzles, the next step was to attempt to correlate their performances empirically. The first property investigated was the velocity. Figure 20 shows the velocities at the 1.0” axial position for all three pressures. Figures 19 and 20 are similar plots for the 0.5” and 0.375” axial positions respectively.

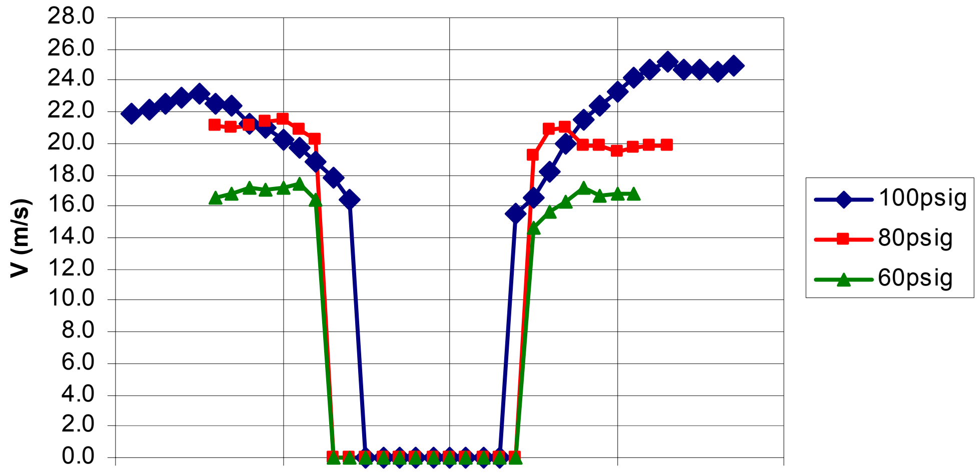

Figure 20. Velocities at 1 inch axial position for three pressures (4 gph).

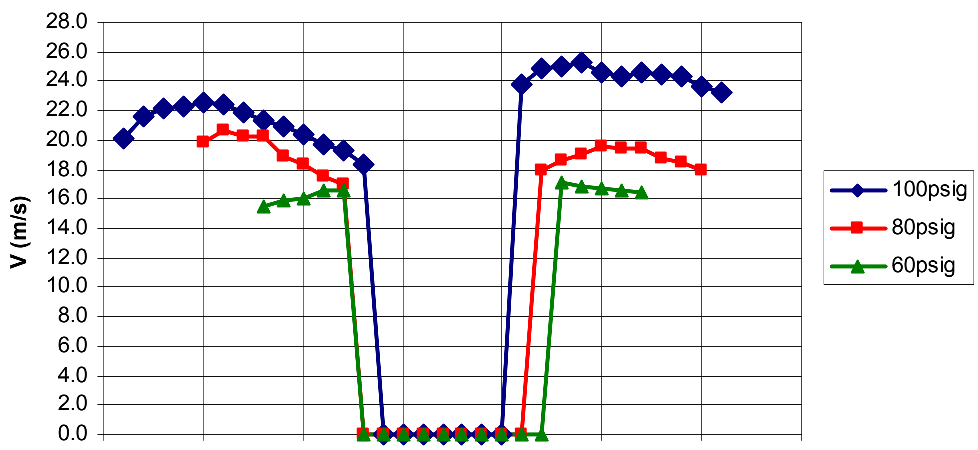

Figure 21. Velocities at 0.5 inch axial position for three pressures (4 gph).

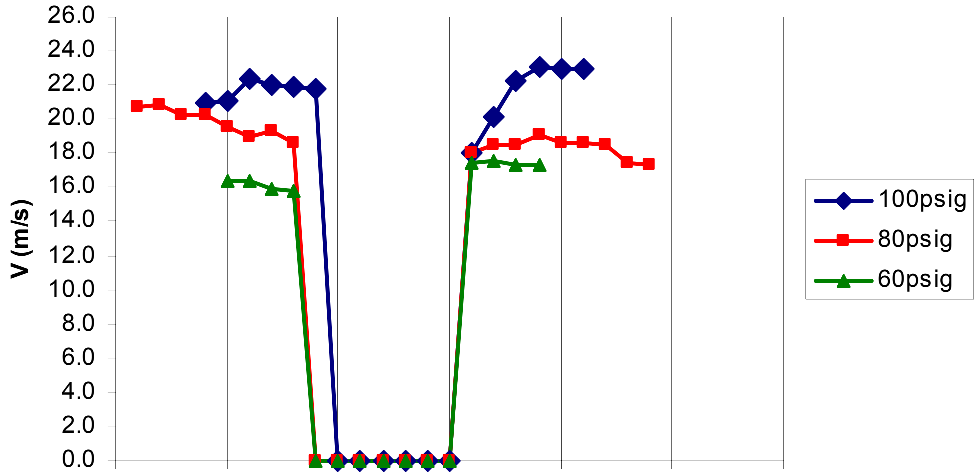

Figure 22. Velocities at 0.375 inch axial position for three pressures (4 gph).

On all three plots, the higher pressure has the highest velocity and the lowest pressure has the lowest. The oil flow at the nozzle exit was assumed to follow Bernoulli's equation, but it was unknown if this relationship would hold through the nozzle itself and continue across the droplet formation. This uncertainty was increased by the internal construction of the nozzle, and the unknown nature of how the spray cone is formed as the oil exits.

If Bernoulli is written to relate the oil nozzle exit velocity (V_e) to the exit stagnation pressure (P_{te}) and the exit static pressure (P_e), then

$$V_e \propto \sqrt{P_{te} - P_e}$$

Since the exit is to vacuum; then

$$\frac{V_e}{\sqrt{P_{te}}} = const. \qquad (1)$$

Clearly V_e is not necessarily the same as the droplet velocity (V), and P_{te} is lower than the stagnation pressure (P_t) measured in the feed line to the nozzle. Nevertheless, a correlation of the measurements in terms of

$$\frac{V}{\sqrt{\delta}} \equiv V_{ref} \tag{2}$$

was examined, where

$$\delta \equiv \frac{P_t}{P_{tref}} \tag{3}$$

and where P_{tref} is a chosen reference stagnation pressure. The reference pressure used in the present study was 100 psia. The results of referencing the velocity data at each axial position are shown in Figures 23 through 25.

Also included in Figures 23 through 25 is a representation of the position of each point within the hollow spray cone. Each data point is shown plotted versus (α), which is a fraction of the spray cone angle from its inner edge to its outer edge. The equation used, with φ being the flow angle at the data point and φ_i and φ_o being the innermost and outermost angles of the spray cone respectively, is

$$\alpha = \frac{\varphi - \varphi_i}{\varphi_o - \varphi_i} \tag{4}$$

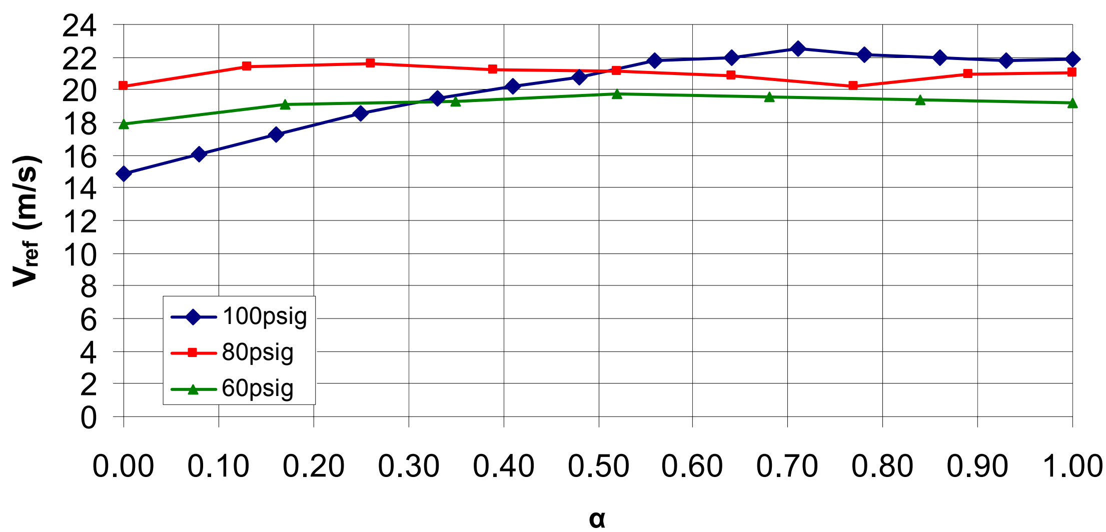

Figure 23. Referenced velocity at 1” axial position for three pressures (4 gph).

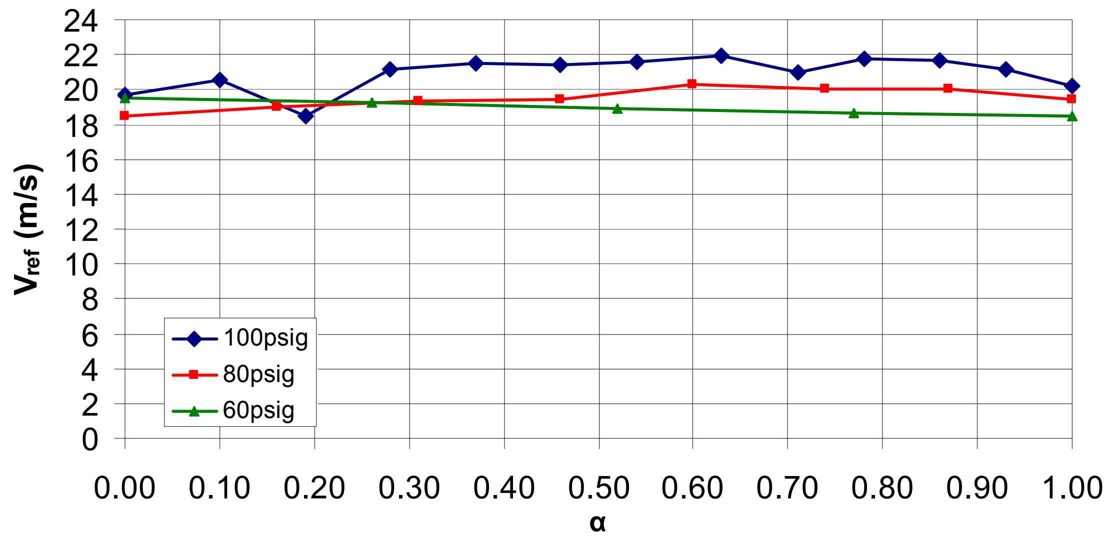

Figure 24. Referenced velocity at 0.5” axial position for three pressures (4 gph).

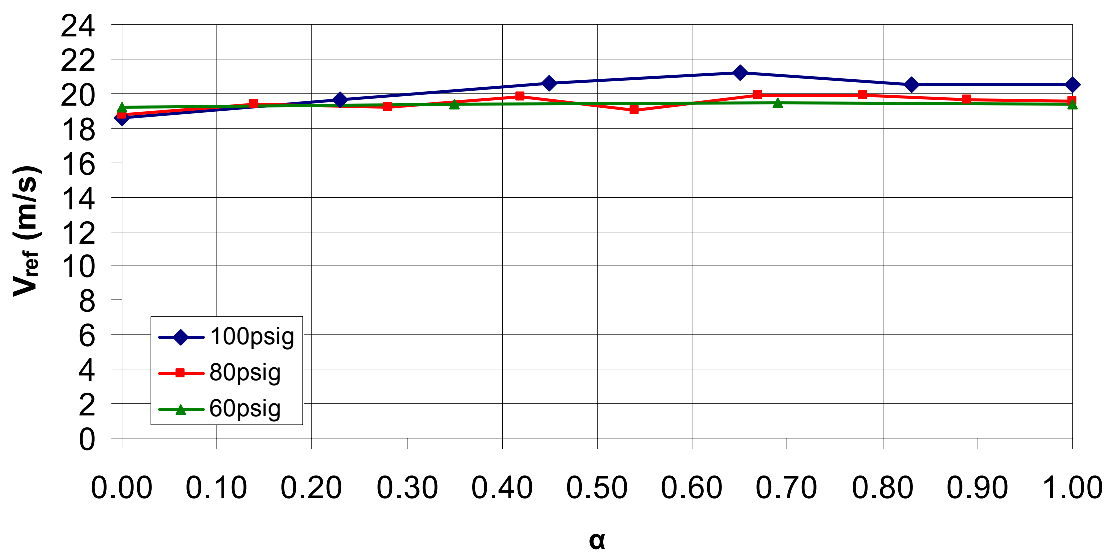

Figure 25. Referenced velocity at 0.375” axial position for three pressures (4 gph).

These three plots probably show the most significant finding of the present study. In all three figures, the referenced velocity is seen to be constant and independent of pressure or axial position in the flow. According to the graphs, V_{ref} is very close to 20 m/s and is a constant throughout the region occupied by the spray.

2. Flow Angle Reduction

It was noted previously, from the data in Figure 15, that the mist cone width widened as the nozzle supply pressure increased. The spread (Δ) of the mist cone with pressure, that is, the difference between the angles of the inner and outer boundaries at each pressure,

$$\Delta = \varphi_o - \varphi_i \tag{5}$$

is shown plotted in Figure 26.

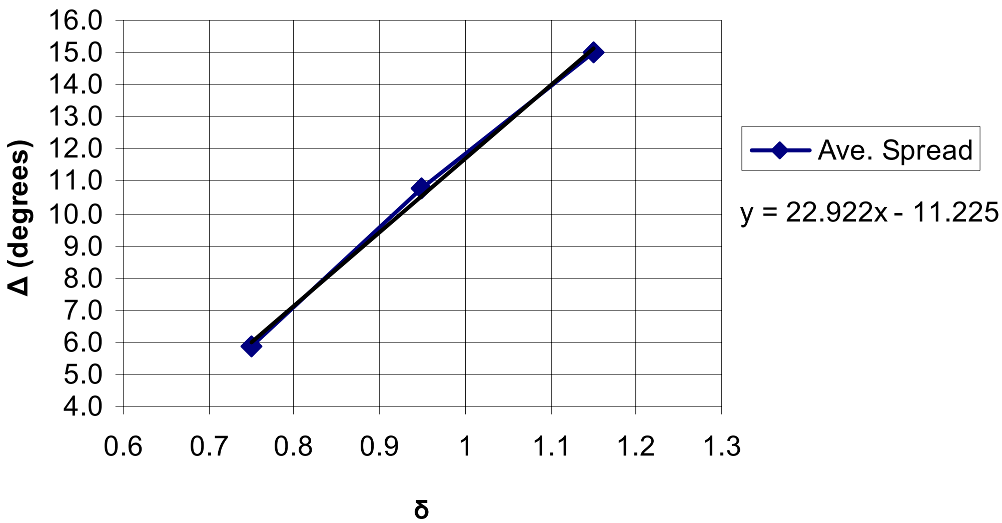

Figure 26. Flow angle spread with non-dimensionalized pressure (4 gph).

Figure 26 shows the nearly linear relationship between the average spread of the spray cone and the supply pressure. A trend line has been added, giving the result

$$\Delta = 22.922\delta - 11.225 \tag{6}$$

3. Flow Rate Reduction

Like the velocity, the flow rate data were referenced to the flow rate that results from an absolute pressure of 100 psia (P_{tref}). The reference pressure flow rate (G_{ref}) was calculated using the relationship between stagnation pressure and flow rate given in Figure 16. The measured flow rates (G) were divided by G_{ref} and plotted versus δ as seen in Figure 27. Figure 27 shows a nearly linear relationship and consequently a trend line was added, giving the result,

$$\frac{G}{G_{ref}} = 0.42263\delta + 0.5725 \qquad (7)$$

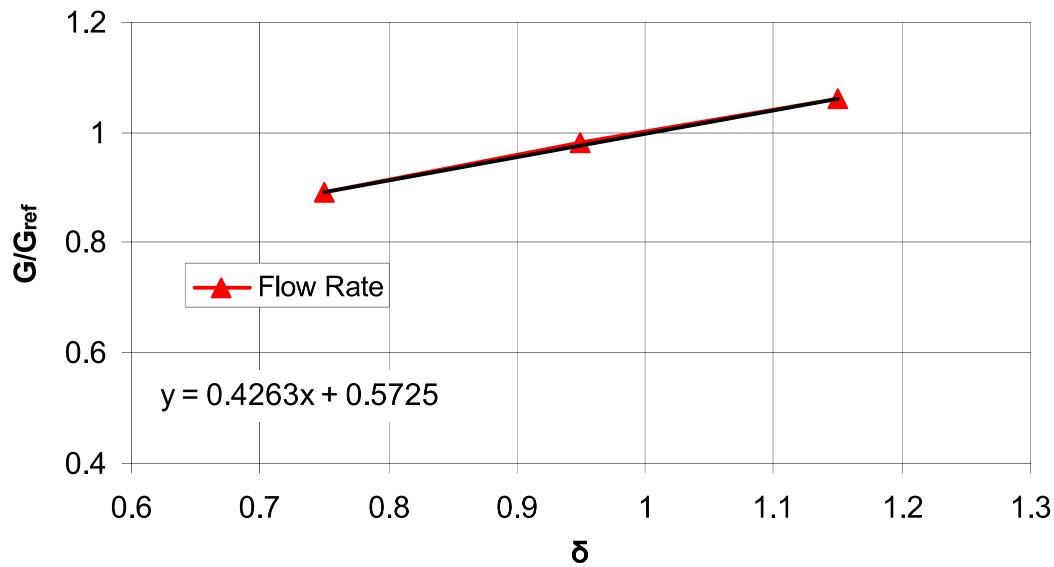

Figure 27. Referenced flow rate, G/G_{ref} variation with non-dimensionalized pressure of the 4 gph nozzle.

4. Summary

The 4 gph "mini-mist" nozzle flow pattern was described quantitatively by the expressions

$$V_{ref} = \frac{V}{\sqrt{\delta}} = const., \text{ where } \delta \equiv \frac{P_t}{P_{tref}}$$

$\Delta = \varphi_o - \varphi_i = a\delta + b$, where a and b are constants.

$$\varphi_m = \frac{\varphi_o - \varphi_i}{2} = const.$$

and the flow rate (G) was described by

$\frac{G}{G_{ref}} = c\delta + d$, where c and d are constants, and G_{ref} is the flow rate at P_{tref}.

For the 4 gph nozzle, using P_{tref} = 100 psia, the following values were found:

$V_{ref} = 20$ (m/s)

$a = 22.922$

$b = -11.225$

$\varphi_m = 32°$

$c = 0.4226$

$d = 0.5725$

B. SIX GALLON PER HOUR NOZZLE

1. Velocity Reduction

A similar data reduction process was attempted for the Hago 6 gph "standard" nozzle as was achieved with the 4 gph "mini mist" nozzle. The results were not as consistent. First, the same reference velocity reduction based on the Bernoulli relationship was attempted. The results are shown in Figures 28, 29, and 30. It is plain that the velocity data did not collapse as well as those produced from the 4 gph nozzle data. One reason is the larger variation in velocities measured at each axial position. This results in "u" shaped curves describing a 'solid cone' spray pattern at each axial station.

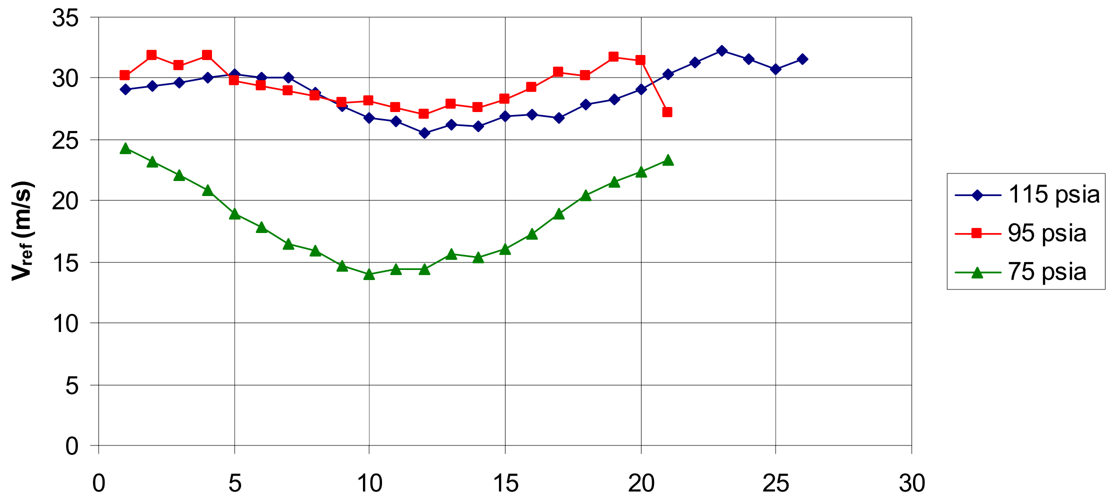

Figure 28. Referenced velocity at 1” axial position for three pressures (6 gph).

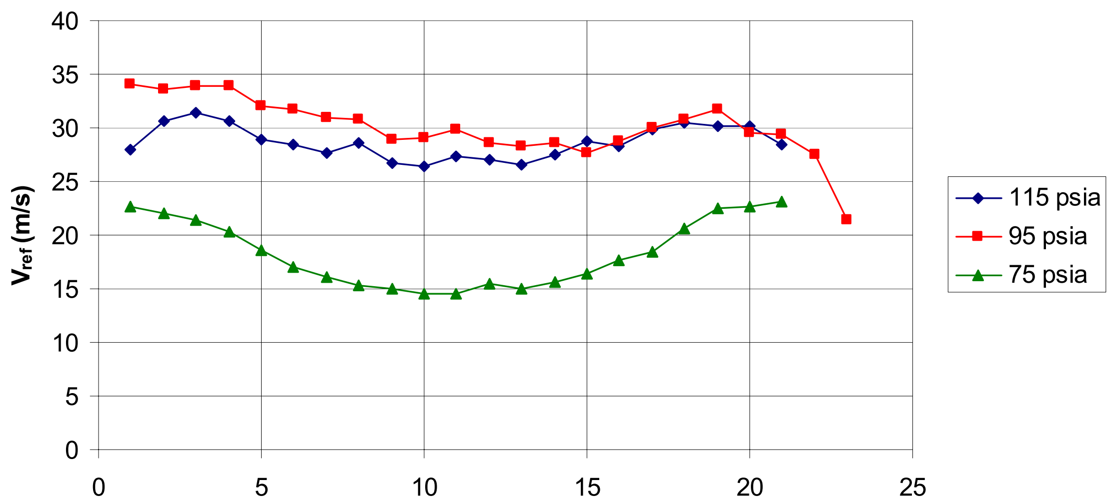

Figure 29. Referenced velocity at 0.5” axial position for three pressures (6 gph).

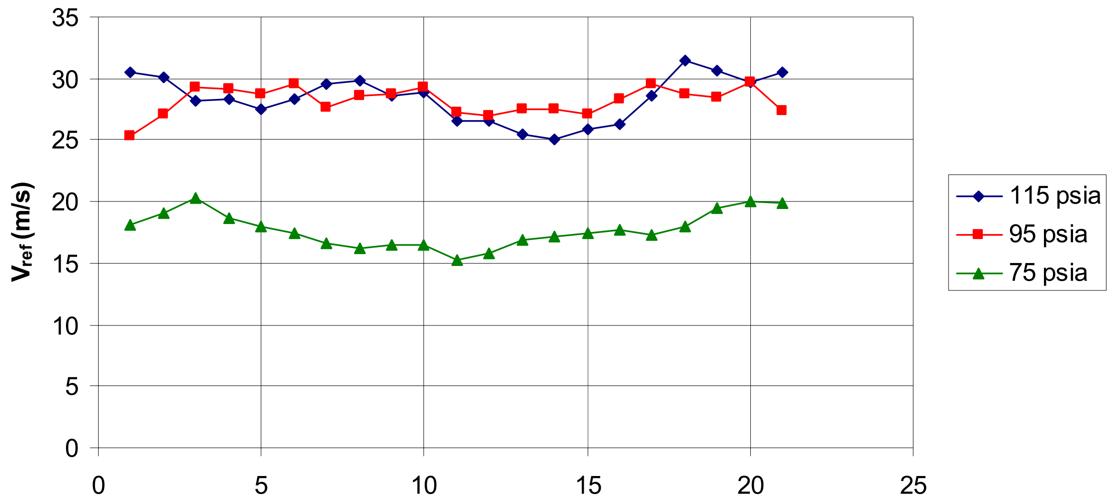

Figure 30. Referenced velocity at 0.25" axial position for three pressures (6 gph).

What is interesting is that the low pressure (60 psig.) curve at each axial position has an average value less than and approaching 20 m/s, similar to the curves generated from the 4 gph data. On the other hand, the 80 and 100 psig curves are very close together but seem to average closer to 25-30 m/s. The previously noted difference in the flow structure that occurred between the 60 psig survey and the 80 and 100 psig may be relevant to explaining this difference. Visually, the 6 gph nozzle spray was a mist at 60 psig (as was the 4 gph nozzle at all test pressures) but contained liquid streaks at the two higher pressures.

2. Temperature Effects

During the course of the study it became apparent that the temperature of the oil was having an effect on how the 6 gph nozzle performed. This was initially observed while warming the system up and observing the flow structure of the 6 gph nozzle as the oil temperature rose from room temperature to its steady operating temperature, a roughly 15 degree Fahrenheit increase.

Photographs were taken of the 6 gph nozzle in operation at various pressures at two different temperatures. The results are shown in Figures 31-35. Because the temperature could not be directly controlled, a very short time window existed for taking pictures at a low (room) temperature, and the highest temperature was the result of the steady operation of the oil pump. This is why the two temperatures in each set of pictures are only 6 degrees apart. Even with this small difference, changes in the structure are evident. Pictures were taken using a five mega-pixel Olympus digital camera.

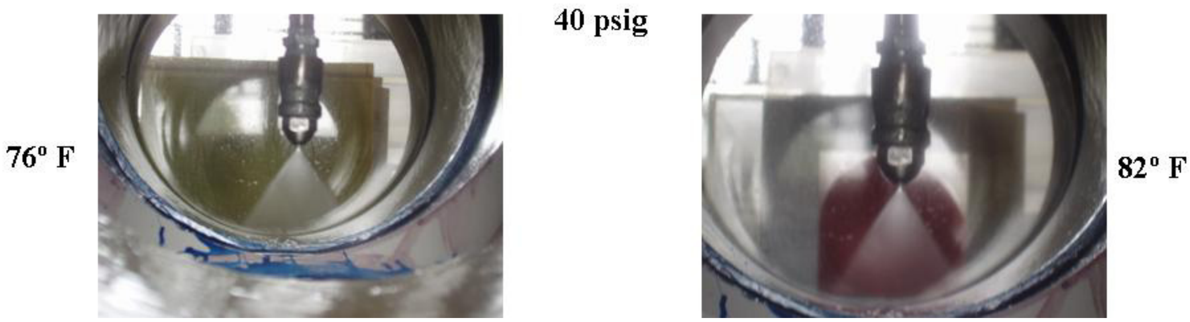

Figure 31. Temperature effect pictures: 6 gph at 40 psig.

Figure 31 shows the lowest gauge pressure at which the nozzle produced a fine mist. At both the upper and lower temperatures the flow looks to be very uniform, having a fog like appearance.

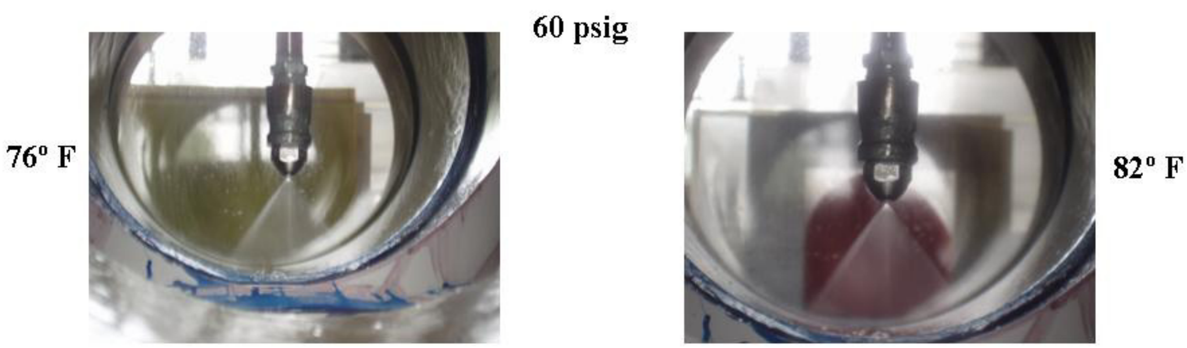

Figure 32. Temperature effect pictures: 6 gph at 60 psig.

Figure 32 shows an increase in the pressure to 60 psig. Still, the nozzle exhibited a uniform structure, but there is clearly a difference between the pictures from the lower and higher temperatures. In the low temperature picture, the left side of the spray shows the beginning of streaks forming. This is not present in the photograph at the higher temperature.

80 psig

76° F **82° F**

Figure 33. Temperature effect pictures: 6 gph at 80 psig.

An increase in pressure to 80 psig is shown in Figure 33. Notice that at the lower temperature, there is a definite non-uniform appearance to the flow not present at lower pressures. This trend seems slightly less apparent in the higher temperature picture.

100 psig

76° F **82° F**

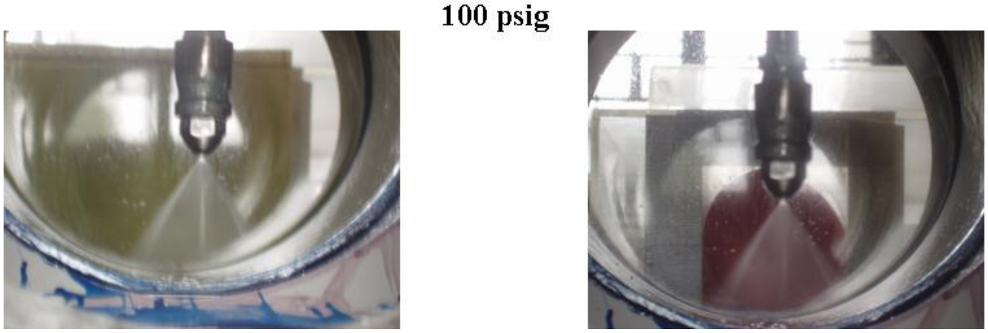

Figure 34. Temperature effect pictures: 6 gph at 100 psig.

Figure 34 shows the nozzle at 100 psig supply pressure. At this pressure the nozzle definitely has a non-uniform structure and it appears that the spray cone has begun to collapse to a smaller outer angle. The temperature difference had only a slight effect on the flow structure.

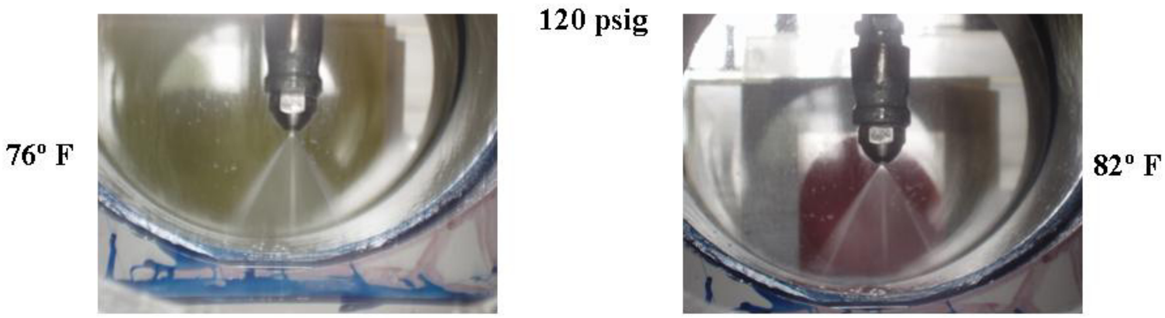

Figure 35. Temperature effect pictures: 6 gph at 120 psig.

Figure 35 shows the pressure increased to 120 psig. At this pressure, the spray cone is seen to be definitely collapsed and the flow is non-uniform. Streaks are very apparent on the edges of the spray cone. As in Figure 34, the temperature difference had little to no effect.

The above photographs show that there is very definitely a temperature effect on the spray structure. Two trends are evident. First, as the pressure was increased, the flow became less steady. It went from fairly uniform to non-uniform over a 20 psig range at a given temperature. Secondly, an increase in temperature at a given pressure helped to make the flow more uniform. This can be seen in both the 60 and 80 psig picture sets. This second trend suggests that if temperature could be further increased it might be possible to run the nozzle at very high pressures with a uniform flow structure.

VI. CONCLUSIONS AND RECOMMENDATIONS

A. CONCLUSIONS

The vacuum test chamber was modified to better suit the flow mapping of mist nozzles using LDV. Two mist nozzles were tested and it was found that while the 4 gph mini mist nozzle exhibited a hollow cone geometry, the 6 gph nozzle was not hollow. Furthermore, previous visual observations of the two nozzles were confirmed regarding their structure. While the 4 gph nozzle created a uniform mist over a large pressure range, the 6 gph nozzle exhibited a very non-uniform flow structure at higher pressures.

For the 4 gph nozzle, all parameters required to quantify the spray, were established relative to the supply pressure. A reference velocity of 20 m/s was found and flow angle spread and flow rate were both quantified with respect to non-dimensionalized pressure. The data from the 6 gph nozzle did not produce similarly consistent results.

The oil temperature did not seem to affect the structure of the 4 gph mini mist nozzle, but did affect the structure of the 6 gph nozzle. Data for the effect of temperature on the viscosity and surface tension of the oil were not available. Both of these parameters could have an effect on the performance of an oil mist nozzle.

B. RECOMMENDATIONS

The flow rate and angle relationships developed from the 4 gph nozzle data are based on only three data points. Surveys should be conducted at lower and higher pressures if the nozzle is to be used outside the pressure range covered in the present study.

Further work is required to better understand how oil temperature affects the flow pattern produced by oil-mist nozzles. This will require the addition of a control on the temperature of the oil in the system (a heating tape can be used to increase the oil temperature). The ability to increase the temperature should be used to investigate the 6 gph "standard" nozzle more extensively. It may be possible to find a temperature and pressure combination that allows the nozzle to spray uniformly, free of streaks.

The LDV system used in the present study measured only two components of the oil droplet velocity. In reality the spray is a three dimensional flow. The nozzles actually produce a swirling flow pattern. In the future, two two-component LDV surveys need to be taken by traversing axially, normal to the chamber window, through the center of the spray. This will add the swirl velocity component present in the flow to the axial and transverse velocities components that were presented here.

APPENDIX A: MSDS FOR MARCOL 5

7332901-00 MARCOL 5
MATERIAL SAFETY DATA BULLETIN

----

1. PRODUCT AND COMPANY IDENTIFICATION

PRODUCT NAME: MARCOL 5
SUPPLIER: EXXON MOBIL CORPORATION
3225 GALLOWS RD.
FAIRFAX, VA 22037

24 - Hour Health and Safety Emergency (call collect): 609-737-4411
24 - Hour Transportation Emergency (Primary) CHEMTREC: 800-424-9300
(Secondary) 281-834-3296
Product and Technical Information:
Lubricants and Specialties: 800-662-4525 800-443-9966
Fuels Products: 800-947-9147
MSDS Fax on Demand: 713-613-3661
MSDS Internet Website: http://www.exxon.com, http://www.mobil.com

----

2. COMPOSITION/INFORMATION ON INGREDIENTS

CHEMICAL NAMES AND SYNONYMS: WHITE MINERAL OIL (PETROLEUM)

GLOBALLY REPORTABLE MSDS INGREDIENTS:

None.

OTHER INGREDIENTS:

Substance Name	Approx. Wt%
WHITE MINERAL OIL (PETROLEUM) (8042-47-5)	100

See Section 8 for exposure limits (if applicable).

----

3. HAZARDS IDENTIFICATION

Under normal conditions of use, this product is not considered hazardous according to regulatory guidelines (See section 15).

EMERGENCY OVERVIEW: Clear Water White Liquid. DOT ERG No. : NA

POTENTIAL HEALTH EFFECTS: Low viscosity material - if swallowed may enter lungs and cause lung damage. Excessive exposure may result in eye, gastrointestinal, or respiratory irritation.

For further health effects/toxicological data, see Section 11.

----

4. FIRST AID MEASURES

EYE CONTACT: Flush thoroughly with water. If irritation occurs, call a physician.
SKIN CONTACT: Wash contact areas with soap and water. Remove and clean oil soaked clothing daily and wash affected area. (See Section 16 - Injection Injury)
INHALATION: Not expected to be a problem. However, if respiratory irritation, dizziness, nausea, or unconsciousness occurs due to excessive vapor or mist exposure, seek immediate medical assistance. If breathing has stopped, assist ventilation with a mechanical device or mouth-to-mouth resuscitation.
INGESTION: Seek immediate medical attention. Do not induce vomiting.
NOTE TO PHYSICIANS: Material if aspirated into the lungs may cause chemical pneumonitis.

----

5. FIRE-FIGHTING MEASURES

EXTINGUISHING MEDIA: Carbon dioxide, foam, dry chemical and water fog.
SPECIAL FIRE FIGHTING PROCEDURES: Water or foam may cause frothing. Use water to keep fire exposed containers cool. Water spray may be used to flush spills away from exposure. Prevent runoff from fire control or dilution from entering streams, sewers, or drinking water supply.
SPECIAL PROTECTIVE EQUIPMENT: For fires in enclosed areas, fire fighters must use self-contained breathing apparatus.
UNUSUAL FIRE AND EXPLOSION HAZARDS: None.
COMBUSTION PRODUCTS: Fumes, smoke, carbon monoxide, sulfur oxides, aldehydes and other decomposition products, in the case of incomplete combustion.
Flash Point C(F): 154(310) (ASTM D-92).
Flammable Limits (approx.% vol.in air) - LEL: 0.9%, UEL: 7.0%
NFPA HAZARD ID: Health: 0, Flammability: 1, Reactivity: 0

----

6. ACCIDENTAL RELEASE MEASURES

NOTIFICATION PROCEDURES: Report spills/releases as required to appropriate authorities. U.S. Coast Guard and EPA regulations require immediate reporting of spills/releases that could reach any waterway including intermittent dry creeks. Report spill/release to Coast Guard National Response Center toll free number (800)424-8802. In case of accident or road spill notify CHEMTREC (800) 424-9300.
PROCEDURES IF MATERIAL IS RELEASED OR SPILLED:
LAND SPILL: Shut off source taking normal safety precautions. Take

measures to minimize the effects on ground water. Recover by pumping or contain spilled material with sand or other suitable absorbent and remove mechanically into containers. If necessary, dispose of adsorbed residues as directed in Section 13.
WATER SPILL: Confine the spill immediately with booms. Warn other ships in the vicinity. Notify port and other relevant authorities. Remove from the surface by skimming or with suitable absorbents. If permitted by regulatory authorities the use of suitable dispersants should be considered where recommended in local oil spill procedures.

ENVIRONMENTAL PRECAUTIONS: Prevent material from entering sewers, water sources or low lying areas; advise the relevant authorities if it has, or if it contaminates soil/vegetation.

PERSONAL PRECAUTIONS: See Section 8

----

7. HANDLING AND STORAGE

HANDLING: No special precautions are necessary beyond normal good hygiene practices. See Section 8 for additional personal protection advice when handling this product.

STORAGE: Keep containers closed when not in use. Do not store in open or unlabelled containers. Store away from strong oxidizing agents and combustible materials. Do not store near heat, sparks, flame or strong oxidants.

SPECIAL PRECAUTIONS: Prevent small spills and leakages to avoid slip hazard.

EMPTY CONTAINER WARNING: Empty containers retain residue (liquid and/or vapor) and can be dangerous. DO NOT PRESSURIZE, CUT, WELD, BRAZE, SOLDER, DRILL, GRIND OR EXPOSE SUCH CONTAINERS TO HEAT, FLAME, SPARKS, STATIC ELECTRICITY, OR OTHER SOURCES OF IGNITION; THEY MAY EXPLODE AND CAUSE INJURY OR DEATH. Do not attempt to refill or clean container since residue is difficult to remove. Empty drums should be completely drained, properly bunged and promptly returned to a drum reconditioner. All containers should be disposed of in an environmentally safe manner and in accordance with governmental regulations.

----

8. EXPOSURE CONTROLS/PERSONAL PROTECTION

OCCUPATIONAL EXPOSURE LIMITS:

When mists/aerosols can occur, the following are recommended: 5 mg/m3 (as oil mist)- ACGIH Threshold Limit Value (TLV), 10 mg/m3 (as oil mist) - ACGIH Short Term Exposure Limit (STEL), 5 mg/m3 (as oil mist) - OSHA Permissible Exposure Limit (PEL)

VENTILATION: If mists are generated, use adequate ventilation, local exhaust or enclosures to control below exposure limits.

RESPIRATORY PROTECTION: If mists are generated, and/or when ventilation is not adequate, wear approved respirator.

EYE PROTECTION: If eye contact is likely, safety glasses with side shields or chemical type goggles should be worn.

SKIN PROTECTION: If prolonged or repeated skin contact is likely, oil impervious gloves should be worn. Good personal hygiene practices should always be followed.

----

9. PHYSICAL AND CHEMICAL PROPERTIES

Typical physical properties are given below. Consult Product Data Sheet for specific details.

APPEARANCE: Liquid
COLOR: Clear Water White
ODOR: Odorless
ODOR THRESHOLD-ppm: NE
pH: NA
BOILING POINT C(F): NE
MELTING POINT C(F): NA
FLASH POINT C(F): 154(310) (ASTM D-92)
FLAMMABILITY (solids): NE
AUTO FLAMMABILITY C(F): NE
EXPLOSIVE PROPERTIES: NA
OXIDIZING PROPERTIES: NA
VAPOR PRESSURE-mmHg 20 C: < 0.1
VAPOR DENSITY: > 2.0
EVAPORATION RATE: NE
RELATIVE DENSITY, 15/4 C: 0.84
SOLUBILITY IN WATER: Negligible
PARTITION COEFFICIENT: > 3.5
VISCOSITY AT 40 C, cSt: 8.0
VISCOSITY AT 100 C, cSt: NE
POUR POINT C(F): -9(15)
FREEZING POINT C(F): NE
VOLATILE ORGANIC COMPOUND: NE
DMSO EXTRACT, IP-346 (WT.%): <3
NA=NOT APPLICABLE NE=NOT ESTABLISHED D=DECOMPOSES

FOR FURTHER TECHNICAL INFORMATION, CONTACT YOUR MARKETING REPRESENTATIVE

----

10. STABILITY AND REACTIVITY

STABILITY (THERMAL, LIGHT, ETC.): Stable.
CONDITIONS TO AVOID: Extreme heat and high energy sources of ignition.
INCOMPATIBILITY (MATERIALS TO AVOID): Strong oxidizers.
HAZARDOUS DECOMPOSITION PRODUCTS: Product does not decompose at ambient temperatures.
HAZARDOUS POLYMERIZATION: Will not occur.

----

11. TOXICOLOGICAL DATA

---ACUTE TOXICOLOGY---

ORAL TOXICITY (RATS): Practically non-toxic (LD50: greater than 2000 mg/kg). ---Based on testing of similar products and/or the components.
DERMAL TOXICITY (RABBITS): Practically non-toxic (LD50: greater than

2000 mg/kg). ---Based on testing of similar products and/or the components.

INHALATION TOXICITY (RATS): Practically non-toxic (LC50: greater than 5 mg/l). ---Based on testing of similar products and/or the components.

EYE IRRITATION (RABBITS): Practically non-irritating. (Draize score: 0 or greater but 6 or less). ---Based on testing of similar products and/or the components.

SKIN IRRITATION (RABBITS): Practically non-irritating. (Primary Irritation Index: 0.5 or less). ---Based on testing of similar products and/or the components.

---REPRODUCTIVE TOXICOLOGY (SUMMARY)---

Oral exposure of pregnant rats to white mineral oil did not cause adverse effects in either the mothers or their offspring.

---CHRONIC TOXICOLOGY (SUMMARY)---

Repeated and/or prolonged exposure may cause irritation to the eyes or respiratory tract. Overexposure to oil mist may result in oil droplet deposition and/or granuloma formation. This product is severely solvent refined and/or severely hydrotreated. Chronic mouse skin painting studies of white mineral oils showed no evidence of carcinogenic effects.

---SENSITIZATION (SUMMARY)---

Not expected to be sensitizing based on tests of this product, components, or similar products.

---OTHER TOXICOLOGY DATA---

Low viscosity white oils have been tested in sensitive rat species (Fischer 344) and after feeding relatively high doses (2% of diet) for 90 days, displayed some minimal hematological changes and liver microgranuloma. Similar effects were not observed to the same degree in other rodent strains or in other species. Medium to high viscosity white oils have been tested in numerous subchronic and chronic feeding, dermal, and inhalation toxicity studies. A number of test species and strains have been used, and most of the studies have shown minimal to no toxicities. Oil that is absorbed is retained in various tissues to some degree, but no clinical disease has been observed in the animal tests. Multiple chronic studies did not show any chronic toxicity, cancer, or reproductive effects. Humans exposed to white oils with biopsy/autopsy evaluations have confirmed the presence of oil in tissues with no clinical disease or long term effect on health. ***Meets requirements of European Pharmacopoeia*** ***Meets requirements of U.S. Pharmacopoeia XXIII***

----

12. ECOLOGICAL INFORMATION

ENVIRONMENTAL FATE AND EFFECTS:

ECOTOXICITY: Available ectoxicity data (LL50 >1000 mg/L) indicates that adverse effects to aquatic organisms are not expected from this product.

MOBILITY: When released into the environment, adsorption to sediment and soil will be the predominant behavior.

PERSISTENCE AND DEGRADABILITY: This product is expected to be inherently biodegradable.

BIOACCUMULATIVE POTENTIAL: Bioaccumulation is unlikely due to the very low water solubility of this product, therefore bioavailability to aquatic organisms is minimal.

----

13. DISPOSAL CONSIDERATIONS

WASTE DISPOSAL: Product is suitable for burning in an enclosed, controlled burner for fuel value. Such burning may be limited pursuant to the Resource Conservation and Recovery Act. In addition, the product is suitable for processing by an approved recycling facility or can be disposed of at an appropriate government waste disposal facility. Use of these methods is subject to user compliance with applicable laws and regulations and consideration of product characteristics at time of disposal.

RCRA INFORMATION: The unused product, in our opinion, is not specifically listed by the EPA as a hazardous waste (40 CFR, Part 261D), nor is it formulated to contain materials which are listed hazardous wastes. It does not exhibit the hazardous characteristics of ignitability, corrosivity, or reactivity. The unused product is not formulated with substances covered by the Toxicity Characteristic Leaching Procedure (TCLP). However, used product may be regulated.

----

14. TRANSPORT INFORMATION

USA DOT: NOT REGULATED BY USA DOT.

RID/ADR: NOT REGULATED BY RID/ADR.

IMO: NOT REGULATED BY IMO.

IATA: NOT REGULATED BY IATA.

STATIC ACCUMULATOR (50 picosiemens or less): YES

----

15. REGULATORY INFORMATION

US OSHA HAZARD COMMUNICATION STANDARD: Product assessed in accordance with OSHA 29 CFR 1910.1200 and determined not to be hazardous.

EU Labeling: Product is not dangerous as defined by the European Union Dangerous Substances/Preparations Directives.

Symbol: Not applicable.

Risk Phrase(s): Not applicable.

Safety Phrase(s): S62.
If swallowed, do not induce vomiting: seek medical advice immediately and show this container or label.

Governmental Inventory Status: All components comply with TSCA and METI.

U.S. Superfund Amendments and Reauthorization Act (SARA) Title III:
This product contains no "EXTREMELY HAZARDOUS SUBSTANCES".

SARA (311/312) REPORTABLE HAZARD CATEGORIES: None.

This product contains no chemicals subject to the supplier notification requirements of SARA (313) toxic release program.

THIS PRODUCT MEETS THE REQUIREMENTS OF FDA REGULATIONS(S): 172.878 178.3620(a)

The following product ingredients are cited on the lists below:

CHEMICAL NAME	CAS NUMBER	LIST CITATIONS *
-------------	----------	--------------

*** NO REPORTABLE INGREDIENTS ***

--- REGULATORY LISTS SEARCHED ---

1=ACGIH ALL	6=IARC 1	11=TSCA 4	16=CA P65 CARC	21=LA RTK
2=ACGIH A1	7=IARC 2A	12=TSCA 5a2	17=CA P65 REPRO	22=MI 293
3=ACGIH A2	8=IARC 2B	13=TSCA 5e	18=CA RTK	23=MN RTK
4=NTP CARC	9=OSHA CARC	14=TSCA 6	19=FL RTK	24=NJ RTK
5=NTP SUS	10=OSHA Z	15=TSCA 12b	20=IL RTK	25=PA RTK
		26=RI RTK		

* EPA recently added new chemical substances to its TSCA Section 4 test rules. Please contact the supplier to confirm whether the ingredients in this product currently appear on a TSCA 4 or TSCA 12b list.
Code key:CARC=Carcinogen; SUS=Suspected Carcinogen; REPRO=Reproductive

----
16. OTHER INFORMATION

USE: MULTI-PURPOSE MINERAL OIL

NOTE: PRODUCTS OF EXXON MOBIL CORPORATION AND ITS AFFILIATED COMPANIES ARE NOT FORMULATED TO CONTAIN PCBS.

Health studies have shown that many hydrocarbons pose potential human health risks which may vary from person to person. Information provided on this MSDS reflects intended use. This product should not be used for other applications. In any case, the following advice should be considered:
INJECTION INJURY WARNING: If product is injected into or under the skin,

or into any part of the body, regardless of the appearance of the wound or its size, the individual should be evaluated immediately by a physician as a surgical emergency. Even though initial symptoms from high pressure injection may be minimal or absent, early surgical treatment within the first few hours may significantly reduce the ultimate extent of injury.

Precautionary Label Text:

WARNING!

LOW VISCOSITY MATERIAL-IF SWALLOWED, MAY BE ASPIRATED AND CAN CAUSE SERIOUS OR FATAL LUNG DAMAGE. EXCESSIVE EXPOSURE MAY RESULT IN EYE, GASTROINTESTINAL, OR RESPIRATORY IRRITATION.

FIRST AID: In case of contact, wash skin with soap and water. Remove contaminated clothing. Call a physician if irritation persists. Wash or dispose of contaminated clothing. If swallowed, seek immediate medical attention. Do not induce vomiting. Only induce vomiting at the instruction of a physician.

For industrial use only. Not intended or suitable for use in or around a household or dwelling.

Refer to product Material Safety Data Sheet for further safety and health information.

****

For Internal Use Only: MHC: 0* 0* 0* 0* 0*, MPPEC: A, TRN: 7332901-00, CMCS97: 97P849, REQ: PS+C, SAFE USE: L
EHS Approval Date: 13AUG2002

****

Prepared by: ExxonMobil Oil Corporation
Environmental Health and Safety Department, Clinton, USA

APPENDIX B: LDV VELOCITY DATA TABLES

Mist Nozzle Run 28JUL05
Vacuum <100 torr
Nozzle Pressure 100psig
Temp. Average 90deg.

		Axial Position (in) 1		
X-pos. (in)	Y comp. (m/s)	X comp. (m/s)	Total vel. (m/s)	Angle (deg)
0.60	17.4	13.3	21.90	37.4
0.58	18.0	13.0	22.20	35.8
0.56	18.2	13.2	22.48	36.0
0.54	18.8	13.0	22.86	34.7
0.52	19.2	12.9	23.13	33.9
0.50	19.1	12.0	22.56	32.1
0.48	19.1	11.8	22.45	31.7
0.46	18.0	11.3	21.25	32.1
0.44	18.0	10.9	21.04	31.2
0.42	17.3	10.6	20.29	31.5
0.40	16.8	10.4	19.76	31.8
0.38	16.2	9.6	18.83	30.7
0.36	15.2	9.3	17.82	31.5
0.34	13.8	8.9	16.42	32.8
0.32	0.0	0.0	0.00	
0.30	0.0	0.0	0.00	
0.20	0.0	0.0	0.00	
0.10	0.0	0.0	0.00	
0.00	0.0	0.0	0.00	
-0.10	0.0	0.0	0.00	
-0.20	0.0	0.0	0.00	
-0.30	0.0	0.0	0.00	
-0.46	0.0	0.0	0.00	
-0.48	14.0	6.6	15.48	25.2
-0.50	14.6	7.9	16.60	28.4
-0.52	15.8	9.0	18.18	29.7
-0.54	16.9	10.6	19.95	32.1
-0.56	17.8	12.0	21.47	34.0
-0.58	18.0	13.3	22.38	36.5
-0.60	18.3	14.4	23.29	38.2
-0.62	18.7	15.4	24.22	39.5
-0.64	18.2	16.6	24.63	42.4
-0.66	17.8	17.9	25.24	45.2
-0.68	16.5	18.3	24.64	48.0
-0.70	16.0	18.8	24.69	49.6
-0.72	15.6	18.9	24.51	50.5
-0.74	14.6	20.3	25.00	54.3

Table 1. 4 gph mini mist nozzle at 1” axial position and 100 psig.

Mist Nozzle Run 28JUL05
Vacuum <100 torr
Nozzle Pressure 100psig
Temp. Average 90deg.

		Axial Position 0.5		
X-pos. (in)	Y comp. (m/s)	X comp. (m/s)	Total vel. (m/s)	Angle (deg)
0.36	15.1	13.2	20.06	41.2
0.34	16.1	14.5	21.67	42.0
0.32	17.2	13.9	22.11	38.9
0.30	17.7	13.5	22.26	37.3
0.28	18.1	13.4	22.52	36.5
0.26	18.4	12.9	22.47	35.0
0.24	18.1	12.4	21.94	34.4
0.22	17.8	11.8	21.36	33.5
0.20	17.8	10.9	20.87	31.5
0.18	18.0	9.5	20.35	27.8
0.16	17.7	8.8	19.77	26.4
0.14	17.5	8.2	19.33	25.1
0.12	16.6	7.9	18.38	25.4
0.10	0.0	0.0	0.00	
0.05	0.0	0.0	0.00	
0.00	0.0	0.0	0.00	
-0.05	0.0	0.0	0.00	
-0.10	0.0	0.0	0.00	
-0.20	0.0	0.0	0.00	
-0.26	0.0	0.0	0.00	
-0.28	17.1	16.6	23.83	44.1
-0.30	17.5	17.6	24.82	45.2
-0.32	17.8	17.5	24.96	44.5
-0.34	17.9	17.9	25.31	45.0
-0.36	16.8	18.0	24.62	47.0
-0.38	16.0	18.4	24.38	49.0
-0.40	15.4	19.1	24.54	51.1
-0.42	14.4	19.8	24.48	54.0
-0.44	13.3	20.4	24.35	56.9
-0.46	12.3	20.2	23.65	58.7
-0.48	10.4	20.8	23.26	63.4

Table 2. 4 gph mini mist nozzle at 0.5" axial position and 100 psig

Mist Nozzle Run 28JUL05
Vacuum <100 torr
Nozzle Pressure 100psig
Temp. Average 90deg.

		Axial Position 0.25		
X-pos. (in)	Y comp. (m/s)	X comp. (m/s)	Total vel. (m/s)	Angle (deg)
0.22	15.4	14.3	21.02	42.9
0.20	16.0	13.7	21.06	40.6
0.18	17.0	14.6	22.41	40.7
0.16	17.4	13.4	21.96	37.6
0.14	17.7	12.9	21.90	36.1
0.12	18.0	12.3	21.80	34.3
0.10	0.0	0.0	0.00	
0.05	0.0	0.0	0.00	
0.00	0.0	0.0	0.00	
-0.05	0.0	0.0	0.00	
-0.10	0.0	0.0	0.00	
-0.12	0.0	0.0	0.00	
-0.14	14.8	10.3	18.03	34.8
-0.16	15.7	12.7	20.19	39.0
-0.18	16.0	15.5	22.28	44.1
-0.20	16.3	16.4	23.12	45.2
-0.22	15.5	17.0	23.01	47.6
-0.24	14.7	17.7	23.01	50.3

Table 3. 4 gph mini mist nozzle at 0.25” axial position and 100 psig.

Mist Nozzle Run 03AUG05
Vacuum <100 torr
Nozzle Pressure 80psig
Temp. Average 90deg.

		Axial Position (in) 1		
X-pos. (in)	Y comp. (m/s)	X comp. (m/s)	Total vel. (m/s)	Angle (deg)
0.58	16.0	13.8	21.13	40.8
0.56	16.6	12.9	21.02	37.9
0.54	17.3	12.2	21.17	35.2
0.52	18.0	11.6	21.41	32.8
0.50	18.6	10.9	21.56	30.4
0.48	18.0	10.5	20.84	30.3
0.46	17.6	10.0	20.24	29.6
0.44	0.0	0.0	0.00	
0.40	0.0	0.0	0.00	
0.30	0.0	0.0	0.00	
0.20	0.0	0.0	0.00	
0.10	0.0	0.0	0.00	
0.00	0.0	0.0	0.00	
-0.10	0.0	0.0	0.00	
-0.20	0.0	0.0	0.00	
-0.30	0.0	0.0	0.00	
-0.40	0.0	0.0	0.00	
-0.50	0.0	0.0	0.00	
-0.58	0.0	0.0	0.00	
-0.60	16.0	10.6	19.19	33.5
-0.62	16.7	12.5	20.86	36.8
-0.64	16.4	13.2	21.05	38.8
-0.66	14.8	13.3	19.90	41.9
-0.68	14.3	13.8	19.87	44.0
-0.70	13.6	14.0	19.52	45.8
-0.72	13.3	14.5	19.68	47.5
-0.74	13.2	14.9	19.91	48.5
-0.76	12.5	15.4	19.83	50.9

Table 4. 4 gph mini mist nozzle at 1” axial position and 80 psig.

Mist Nozzle Run 03AUG05
Vacuum <100 torr
Nozzle Pressure 80psig
Temp. Average 90deg.

	Axial Position (in) 0.5			
X-pos. (in)	Y comp. (m/s)	X comp. (m/s)	Total vel. (m/s)	Angle (deg)
0.40	15.0	13.0	19.85	40.9
0.38	15.7	13.4	20.64	40.5
0.36	15.6	13.0	20.31	39.8
0.34	15.9	12.5	20.23	38.2
0.32	15.5	10.9	18.95	35.1
0.30	15.7	9.4	18.30	30.9
0.28	15.4	8.3	17.49	28.3
0.26	15.8	6.3	17.01	21.7
0.24	0.0	0.0	0.00	
0.20	0.0	0.0	0.00	
0.10	0.0	0.0	0.00	
0.05	0.0	0.0	0.00	
0.00	0.0	0.0	0.00	
-0.05	0.0	0.0	0.00	
-0.10	0.0	0.0	0.00	
-0.20	0.0	0.0	0.00	
-0.22	0.0	0.0	0.00	
-0.24	14.3	10.8	17.92	
-0.26	14.3	11.9	18.60	
-0.28	14.5	12.4	19.08	40.5
-0.30	14.3	13.3	19.53	42.9
-0.32	14.0	13.4	19.38	43.7
-0.34	13.6	13.8	19.38	45.4
-0.36	12.5	14.0	18.77	48.2
-0.38	11.5	14.4	18.43	51.4
-0.40	10.5	14.6	17.98	54.3

Table 5. 4 gph mini mist nozzle at 0.5” axial and 80 psig.

Mist Nozzle Run 03AUG05
Vacuum <100 torr
Nozzle Pressure 80psig
Temp. Average 90deg.

		Axial Position (in) 0.375		
X-pos. (in)	Y comp. (m/s)	X comp. (m/s)	Total vel. (m/s)	Angle (deg)
0.34	14.3	15.0	20.72	46.4
0.32	14.2	15.2	20.80	46.9
0.30	14.2	14.5	20.30	45.6
0.28	14.7	13.9	20.23	43.4
0.26	14.8	12.7	19.50	40.6
0.24	15.3	11.3	19.02	36.4
0.22	16.1	10.6	19.28	33.4
0.20	16.2	9.2	18.63	29.6
0.18	0.0	0.0	0.00	
0.10	0.0	0.0	0.00	
0.05	0.0	0.0	0.00	
0.00	0.0	0.0	0.00	
-0.05	0.0	0.0	0.00	
-0.10	0.0	0.0	0.00	
-0.12	0.0	0.0	0.00	
-0.14	15.0	10.0	18.03	33.7
-0.16	15.4	10.3	18.53	33.8
-0.18	15.1	10.6	18.45	35.1
-0.20	15.1	11.7	19.10	37.8
-0.22	14.0	12.2	18.57	41.1
-0.24	13.1	13.2	18.60	45.2
-0.26	12.7	13.5	18.53	46.7
-0.28	10.9	13.6	17.43	51.3
-0.30	9.6	14.5	17.39	56.5

Table 6. 4 gph mini mist nozzle at 0.375” axial position and 80 psig.

Mist Nozzle Run 04AUG05
Vacuum <100 torr
Nozzle Pressure 60psig
Temp. Average 88deg.

Axial Position (in) 1				
X-pos. (in)	Y comp. (m/s)	X comp. (m/s)	Total vel. (m/s)	Angle (deg)
0.58	12.2	11.2	16.56	42.6
0.56	12.8	10.9	16.81	40.4
0.54	13.7	10.4	17.20	37.2
0.52	13.9	9.8	17.01	35.2
0.50	14.3	9.5	17.17	33.6
0.48	15.0	9.0	17.49	31.0
0.46	14.1	8.5	16.46	31.1
0.44	0.0	0.0	0.00	
0.40	0.0	0.0	0.00	
0.30	0.0	0.0	0.00	
0.20	0.0	0.0	0.00	
0.10	0.0	0.0	0.00	
0.00	0.0	0.0	0.00	
-0.10	0.0	0.0	0.00	
-0.20	0.0	0.0	0.00	
-0.30	0.0	0.0	0.00	
-0.40	0.0	0.0	0.00	
-0.50	0.0	0.0	0.00	
-0.54	0.0	0.0	0.00	
-0.56	11.6	8.9	14.62	37.5
-0.58	12.1	9.9	15.63	39.3
-0.60	12.2	10.7	16.23	41.3
-0.62	12.8	11.5	17.21	41.9
-0.64	11.5	12.1	16.69	46.5
-0.66	10.8	12.9	16.82	50.1
-0.68	10.2	13.3	16.76	52.5

Table 7. 4 gph mini mist nozzle at 1” axial position and 60 psig.

Mist Nozzle Run 04AUG05
Vacuum <100 torr
Nozzle Pressure 60psig
Temp. Average 88deg.

		Axial Position (in) 0.5		
X-pos. (in)	Y comp. (m/s)	X comp. (m/s)	Total vel. (m/s)	Angle (deg)
0.38	10.2	11.6	15.45	48.7
0.36	11.0	11.4	15.84	46.0
0.34	11.8	10.9	16.06	42.7
0.32	12.5	10.8	16.52	40.8
0.30	12.7	10.7	16.61	40.1
0.28	0.0	0.0	0.00	
0.20	0.0	0.0	0.00	
0.10	0.0	0.0	0.00	
0.05	0.0	0.0	0.00	
0.00	0.0	0.0	0.00	
-0.05	0.0	0.0	0.00	
-0.10	0.0	0.0	0.00	
-0.20	0.0	0.0	0.00	
-0.30	0.0	0.0	0.00	
-0.32	0.0	0.0	0.00	
-0.34	11.6	12.6	17.13	47.4
-0.36	11.4	12.4	16.84	47.4
-0.38	11.0	12.6	16.73	48.9
-0.40	10.2	13.0	16.52	51.9
-0.42	9.9	13.2	16.50	53.1

Table 8. 4 gph mini mist nozzle at 0.5” axial position and 60 psig.

Mist Nozzle Run 04AUG05
Vacuum <100 torr
Nozzle Pressure 60psig
Temp. Average 88deg.

Axial Position (in) 0.375				
X-pos. (in)	Y comp. (m/s)	X comp. (m/s)	Total vel. (m/s)	Angle (deg)
0.28	11.3	11.8	16.34	46.2
0.26	11.8	11.4	16.41	44.0
0.24	11.6	10.9	15.92	43.2
0.22	11.8	10.5	15.80	41.7
0.20	0.0	0.0	0.00	
0.10	0.0	0.0	0.00	
0.05	0.0	0.0	0.00	
0.00	0.0	0.0	0.00	
-0.05	0.0	0.0	0.00	
-0.10	0.0	0.0	0.00	
-0.20	0.0	0.0	0.00	
-0.22	10.9	13.6	17.43	51.3
-0.24	10.8	13.9	17.60	52.2
-0.26	10.2	14.0	17.32	53.9
-0.28	10.4	13.8	17.28	53.0

Table 9. 4 gph mini mist nozzle at 0.375” axial position and 60 psig.

Mist Nozzle Run 14JUN05
Vacuum <100 torr
Nozzle Pressure 100psig
Temp. Average 78deg.

		Axial Position (in) 1		
X-pos. (in)	Y comp. (m/s)	X comp. (m/s)	Total vel. (m/s)	Angle (deg)
0.80	24.0	20.0	31.24	39.8
0.72	25.1	19.0	31.48	37.1
0.68	26.1	18.2	31.82	34.9
0.64	27.0	17.5	32.18	32.9
0.60	28.0	16.5	32.50	30.5
0.56	28.5	15.1	32.25	27.9
0.52	29.0	14.1	32.25	25.9
0.48	28.0	13.0	30.87	24.9
0.40	27.6	11.2	29.79	22.1
0.32	27.3	8.9	28.71	18.1
0.24	27.6	6.5	28.36	13.3
0.16	27.0	4.4	27.36	9.3
0.08	28.0	2.4	28.10	4.9
0.00	28.0	0.3	28.00	0.6
-0.08	28.7	2.8	28.84	5.6
-0.16	28.6	4.5	28.95	8.9
-0.24	27.9	6.7	28.69	13.5
-0.32	28.6	8.7	29.89	16.9
-0.40	28.4	10.7	30.35	20.6
-0.48	28.4	13.1	31.28	24.8
-0.56	28.7	15.4	32.57	28.2
-0.60	29.1	16.7	33.55	29.9
-0.64	30.0	17.3	34.63	30.0
-0.68	28.6	18.0	33.79	32.2
-0.72	27.1	18.8	32.98	34.8
-0.80	27.0	20.4	33.84	37.1

Table 10. 6 gph mist nozzle at 1” axial position and 100 psig.

Mist Nozzle Run 14JUN05
Vacuum <100 torr
Nozzle Pressure 100psig
Temp. Average 78deg.

Axial Position (in) 0.5				
X-pos. (in)	Y comp. (m/s)	X comp. (m/s)	Total vel. (m/s)	Angle (deg)
0.40	21.3	21.1	29.98	44.7
0.36	26.0	20.0	32.80	37.6
0.32	28.5	17.8	33.60	32.0
0.28	29.2	15.0	32.83	27.2
0.24	28.4	12.3	30.95	23.4
0.20	28.8	10.0	30.49	19.1
0.16	28.5	8.1	29.63	15.9
0.12	30.0	6.5	30.70	12.2
0.08	28.5	3.0	28.66	6.0
0.04	28.2	2.0	28.27	4.1
0.00	29.3	0.4	29.30	0.8
-0.04	29.0	1.8	29.06	3.6
-0.08	28.2	3.4	28.40	6.9
-0.12	28.6	7.3	29.52	14.3
-0.16	29.3	9.5	30.80	18.0
-0.20	28.0	11.8	30.38	22.9
-0.24	28.8	14.1	32.07	26.1
-0.28	28.0	16.8	32.65	31.0
-0.32	27.4	17.1	32.30	32.0
-0.36	27.5	16.9	32.28	31.6
-0.40	26.0	15.9	30.48	31.4

Table 11. 6 gph mist nozzle at 0.5” axial position and 100 psig.

Mist Nozzle Run 14JUN05
Vacuum <100 torr
Nozzle Pressure 100psig
Temp. Average 78deg.

		Axial Position (in) 0.25		
X-pos. (in)	Y comp. (m/s)	X comp. (m/s)	Total vel. (m/s)	Angle (deg)
0.20	27.4	17.9	32.73	33.2
0.18	27.8	16.3	32.23	30.4
0.16	27.2	13.2	30.23	25.9
0.14	28.1	11.4	30.32	22.1
0.12	27.5	10.6	29.47	21.1
0.10	28.8	9.6	30.36	18.4
0.08	30.7	7.7	31.65	14.1
0.06	31.6	5.2	32.02	9.3
0.04	30.6	2.3	30.69	4.3
0.02	30.8	3.8	31.03	7.0
0.00	28.5	1.1	28.52	2.2
-0.02	28.3	2.6	28.42	5.2
-0.04	27.1	3.7	27.35	7.8
-0.06	26.2	5.9	26.86	12.7
-0.08	26.9	6.7	27.72	14.0
-0.10	25.6	11.8	28.19	24.7
-0.12	27.5	13.6	30.68	26.3
-0.14	30.3	14.8	33.72	26.0
-0.16	29.0	15.3	32.79	27.8
-0.18	27.4	16.1	31.78	30.4
-0.20	27.3	18.0	32.70	33.4

Table 12. 6 gph mist nozzle at 0.25” axial position and 100 psig.

Mist Nozzle Run 16JUN05
Vacuum <100 torr
Nozzle Pressure 80psig
Temp. Average 80deg. (max 85)

Axial Position (in)

1				
X-pos. (in)	Y comp. (m/s)	X comp. (m/s)	Total vel. (m/s)	Angle (deg)
-0.90	20.5	21.1	29.42	45.8
-0.81	23.1	20.8	31.08	42.0
-0.72	24.7	17.4	30.21	35.2
-0.63	26.3	16.5	31.05	32.1
-0.54	25.7	13.5	29.03	27.7
-0.45	26.3	11.3	28.62	23.3
-0.35	26.8	9.0	28.27	18.6
-0.27	27.0	6.5	27.77	13.5
-0.18	27.0	4.2	27.32	8.8
-0.09	27.3	2.5	27.41	5.2
0.00	26.9	0.8	26.91	1.7
0.09	26.3	1.7	26.35	3.7
0.18	27.0	3.3	27.20	7.0
0.27	26.3	5.3	26.83	11.4
0.36	26.5	7.4	27.51	15.6
0.45	26.6	10.4	28.56	21.4
0.54	26.4	13.5	29.65	27.1
0.63	25.0	15.6	29.47	32.0
0.72	25.6	17.4	30.95	34.2
0.81	23.6	19.5	30.61	39.6
0.90	20.4	17.0	26.55	39.8

Table 13. 6 gph mist nozzle at 1” axial position and 80 psig.

Mist Nozzle Run 16JUN05
Vacuum <100 torr
Nozzle Pressure 80psig
Temp. Average 80deg. (max 85)

Axial Position (in)				
0.5				
X-pos. (in)	Y comp. (m/s)	X comp. (m/s)	Total vel. (m/s)	Angle (deg)
0.45	22.2	24.7	33.21	48.1
0.40	24.0	22.3	32.76	42.9
0.36	25.6	21.0	33.11	39.4
0.32	27.0	19.0	33.02	35.1
0.28	26.5	16.6	31.27	32.1
0.24	26.8	15.3	30.86	29.7
0.20	27.3	12.8	30.15	25.1
0.16	28.0	10.8	30.01	21.1
0.12	27.9	4.0	28.19	8.2
0.08	28.3	2.0	28.37	4.0
0.04	29.0	1.1	29.02	2.2
0.00	27.9	0.1	27.90	0.2
-0.04	27.6	0.7	27.61	1.5
-0.08	27.8	1.5	27.84	3.1
-0.12	26.9	2.6	27.03	5.5
-0.16	26.6	8.6	27.96	17.9
-0.20	27.0	11.4	29.31	22.9
-0.24	26.9	13.4	30.05	26.5
-0.28	26.5	15.9	30.90	31.0
-0.32	23.7	16.2	28.71	34.4
-0.36	22.5	17.8	28.69	38.3
-0.40	20.0	17.8	26.77	41.7
-0.45	15.9	13.4	20.79	40.1

Table 14. 6 gph mist nozzle at 0.5” axial position and 80 psig.

Mist Nozzle Run 16JUN05
Vacuum <100 torr
Nozzle Pressure 80psig
Temp. Average 80deg. (max 85)

Axial Position (in)				
0.25				
X-pos. (in)	Y comp. (m/s)	X comp. (m/s)	Total vel. (m/s)	Angle (deg)
-0.20	21.9	11.4	24.69	27.5
-0.18	23.9	11.4	26.48	25.5
-0.16	24.2	15.1	28.52	32.0
-0.14	24.2	14.8	28.37	31.4
-0.12	25.0	12.6	28.00	26.7
-0.10	26.7	10.7	28.76	21.8
-0.08	25.4	9.0	26.95	19.5
-0.06	26.8	7.5	27.83	15.6
-0.04	27.5	5.2	27.99	10.7
-0.02	28.2	4.7	28.59	9.5
0.00	26.5	0.3	26.50	0.6
0.02	26.2	2.7	26.34	5.9
0.04	26.4	4.5	26.78	9.7
0.06	26.3	5.2	26.81	11.2
0.08	25.5	6.7	26.37	14.7
0.10	26.3	8.5	27.64	17.9
0.12	26.9	10.4	28.84	21.1
0.14	25.3	11.9	27.96	25.2
0.16	24.6	12.9	27.78	27.7
0.18	24.8	14.8	28.88	30.8
0.20	23.9	12.0	26.74	26.7

Table 15. 6 gph mist nozzle at 0.25” axial position and 80 psig.

Mist Nozzle Run 20JUL05
Vacuum <100 torr
Nozzle Pressure 60psig
Temp. Average 82deg.

		Axial Position (in) 1		
X-pos. (in)	Y comp. (m/s)	X comp. (m/s)	Total vel. (m/s)	Angle (deg)
0.80	11.0	17.9	21.01	58.4
0.72	12.0	16.1	20.08	53.3
0.64	12.4	14.5	19.08	49.5
0.56	12.2	13.3	18.05	47.5
0.48	11.8	11.4	16.41	44.0
0.40	12.2	9.4	15.40	37.6
0.32	11.9	7.8	14.23	33.2
0.24	12.3	6.1	13.73	26.4
0.16	12.0	4.3	12.75	19.7
0.08	11.9	2.5	12.16	11.9
0.00	12.4	0.8	12.43	3.7
-0.08	12.3	2.2	12.50	10.1
-0.16	13.0	4.0	13.60	17.1
-0.24	12.3	5.2	13.35	22.9
-0.32	11.9	7.1	13.86	30.8
-0.40	12.1	8.9	15.02	36.3
-0.48	12.3	10.8	16.37	41.3
-0.56	12.7	12.4	17.75	44.3
-0.64	12.4	14.0	18.70	48.5
-0.72	11.4	15.7	19.40	54.0
-0.80	10.8	17.1	20.22	57.7

Table 16. 6 gph mist nozzle at 1” axial position and 60 psig.

Mist Nozzle Run 20JUL05
Vacuum <100 torr
Nozzle Pressure 60psig
Temp. Average 82deg.

Axial Position (in) 0.5				
X-pos. (in)	Y comp. (m/s)	X comp. (m/s)	Total vel. (m/s)	Angle (deg)
0.40	10.1	16.8	19.60	59.0
0.36	11.2	15.5	19.12	54.1
0.32	11.8	14.3	18.54	50.5
0.28	12.1	12.8	17.61	46.6
0.24	12.0	10.8	16.14	42.0
0.20	11.8	8.8	14.72	36.7
0.16	12.2	6.7	13.92	28.8
0.12	12.3	5.0	13.28	22.1
0.08	12.4	4.0	13.03	17.9
0.04	12.3	2.8	12.61	12.8
0.00	12.5	1.0	12.54	4.6
-0.04	13.1	2.9	13.42	12.5
-0.08	12.4	3.9	13.00	17.5
-0.12	12.3	5.6	13.51	24.5
-0.16	12.2	7.4	14.27	31.2
-0.20	12.3	9.1	15.30	36.5
-0.24	11.6	11.0	15.99	43.5
-0.28	12.0	13.3	17.91	47.9
-0.32	12.1	15.2	19.43	51.5
-0.36	11.0	16.2	19.58	55.8
-0.40	11.0	16.7	20.00	56.6

Table 17. 6 gph mist nozzle at 0.5” axial position and 60 psig.

Mist Nozzle Run 20JUL05
Vacuum <100 torr
Nozzle Pressure 60psig
Temp. Average 82deg.

		Axial Position (in) 0.25		
X-pos. (in)	Y comp. (m/s)	X comp. (m/s)	Total vel. (m/s)	Angle (deg)
0.20	11.0	11.1	15.63	45.3
0.18	10.3	12.9	16.51	51.4
0.16	10.9	13.8	17.59	51.7
0.14	11.3	11.5	16.12	45.5
0.12	11.6	10.4	15.58	41.9
0.10	12.0	9.2	15.12	37.5
0.08	12.3	7.4	14.35	31.0
0.06	12.5	6.5	14.09	27.5
0.04	13.1	5.8	14.33	23.9
0.02	13.3	5.1	14.24	21.0
0.00	13.2	1.0	13.24	4.3
-0.02	13.4	2.8	13.69	11.8
-0.04	14.1	4.0	14.66	15.8
-0.06	14.0	5.0	14.87	19.7
-0.08	13.7	6.2	15.04	24.3
-0.10	13.4	7.4	15.31	28.9
-0.12	12.6	8.2	15.03	33.1
-0.14	11.6	10.4	15.58	41.9
-0.16	11.5	12.3	16.84	46.9
-0.18	10.6	13.7	17.32	52.3
-0.20	10.4	13.7	17.20	52.8

Table 18. 6 gph mist nozzle at 0.25” axial position and 60 psig.

LIST OF REFERENCES

1. Shreeve, R.P., Seivwright, D.L., Hobson, G.V., "HCF Spin-Testing with Oil-Jet Excitation", Proceedings of the 9th National Turbine Engine High Cycle Fatigue (HCF) Conference, Pinehurst, NC, March 16-19, 2004.

2. Shreeve, R.P., Seivwright, D.L., Hobson, G.V. and Moreno, O., "Oil-Jet Excitation in Rotor Spin Testing", Proceedings of the 10th National Turbine Engine High Cycle Fatigue (HCF) Conference, New Orleans, LA, March 8-11, 2005.

3. Moreno, O.R. "Investigation and Development of Oil-Injection Nozzles for High-Cycle Fatigue Rotor Spin Test," Thesis, Naval Postgraduate School, Monterey, CA March 2005.

4. Murray, K.D. "Automation and Extension of LDV Measurement of Off-Design Flow in a Cascade Wind Tunnel," Thesis, Naval Postgraduate School, Monterey, CA June 1989.

THIS PAGE INTENTIONALLY LEFT BLANK

INITIAL DISTRIBUTION LIST

1. Defense Technical Information Center
   Ft. Belvoir, Virginia

2. Dudley Knox Library
   Naval Postgraduate School
   Monterey, California

3. Dr. Raymond Shreeve
   Naval Postgraduate School
   Monterey, California

4. Dr. Garth Hobson
   Naval Postgraduate School
   Monterey, California

5. Raymond Pickering
   Naval Air Systems Command (AIR 4.4)
   Patuxent River, Maryland

6. Frank Lieghley
   USAF AFRL/PRTS
   Wright-Patterson AFB, Ohio

7. Dr. Andy von Flotow
   Hood Technology Corporation
   Hood River, Oregon